This document was prepared by the DUNE collaboration using the resources of the Fermi National Accelerator Laboratory (Fermilab), a U.S. Department of Energy, Office of Science, HEP User Facility. Fermilab is managed by Fermi Research Alliance, LLC (FRA), acting under Contract No. DE-AC02-07CH11359.

The DUNE collaboration also acknowledges the international, national, and regional funding agencies supporting the institutions who have contributed to completing this Technical Design Report.

Authors

B. Abi,[129] R. Acciarri,[56] Mario A. Acero,[8] G. Adamov,[59] D. Adams,[15] M. Adinolfi,[14] Z. Ahmad,[163] J. Ahmed,[166] T. Alion,[153] S. Alonso Monsalve,[18] C. Alt,[49] J. Anderson,[4] C. Andreopoulos,[109] M. P. Andrews,[56] F. Andrianala,[2] S. Andringa,[103] A. Ankowski,[143] J. Anthony,[28] M. Antonova,[72] S. Antusch,[9] A. Aranda Fernandez,[36] A. Ariga,[10] L. O. Arnold,[39] M. A. Arroyave,[48] J. Asaadi,[157] A. Aurisano,[34] V. Aushev,[101] D. Autiero,[81] F. Azfar,[129] H. Back,[130] J. J. Back,[166] C. Backhouse,[161] P. Baesso,[14] L. Bagby,[56] R. Bajou,[1] S. Balasubramanian,[170] P. Baldi,[23] B. Bambah,[70] F. Barao,[103, 105] G. Barenboim,[72] G. J. Barker,[166] W. Barkhouse,[123] C. Barnes,[116] G. Barr,[129] J. Barranco Monarca,[64] N. Barros,[103, 106] J. L. Barrow,[155, 56] A. Bashyal,[128] V. Basque,[114] F. Bay,[122] J. L. Bazo Alba,[137] J. F. Beacom,[127] E. Bechetoille,[81] B. Behera,[38] L. Bellantoni,[56] G. Bellettini,[135] V. Bellini,[74] O. Beltramello,[18] D. Belver,[19] N. Benekos,[18] F. Bento Neves,[104] J. Berger,[136] S. Berkman,[56] P. Bernardini,[144] R. M. Berner,[10] H. Berns,[22] S. Bertolucci,[73] M. Betancourt,[56] Y. Bezawada,[22] M. Bhattacharjee,[86] B. Bhuyan,[86] S. Biagi,[152] J. Bian,[23] M. Biassoni,[76] K. Biery,[56] B. Bilki,[11] M. Bishai,[15] A. Bitadze,[114] A. Blake,[107] B. Blanco Siffert,[55] F. D. M. Blaszczyk,[56] G. C. Blazey,[124] E. Blucher,[32] J. Boissevain,[110] S. Bolognesi,[17] T. Bolton,[98] M. Bonesini,[76] M. Bongrand,[102] F. Bonini,[15] A. Booth,[153] C. Booth,[146] S. Bordoni,[18] A. Borkum,[153] T. Boschi,[47] N. Bostan,[90] P. Bour,[41] S. B. Boyd,[166] D. Boyden,[124] J. Bracinik,[12] D. Braga,[56] D. Brailsford,[107] A. Brandt,[157] J. Bremer,[18] C. Brew,[142] E. Brianne,[114] S. J. Brice,[56] C. Brizzolari,[76] C. Bromberg,[117] G. Brooijmans,[39] J. Brooke,[14] A. Bross,[56] G. Brunetti,[131] N. Buchanan,[38] H. Budd,[140] D. Caiulo,[81] P. Calafiura,[108] J. Calcutt,[117] M. Calin,[16] S. Calvez,[38] E. Calvo,[19] L. Camilleri,[39] A. Caminata,[75] M. Campanelli,[161] D. Caratelli,[56] G. Carini,[15] B. Carlus,[81] P. Carniti,[76] I. Caro Terrazas,[38] H. Carranza,[157] A. Castillo,[145] C. Castromonte,[89] C. Cattadori,[76] F. Cavalier,[102] F. Cavanna,[56] S. Centro,[131] G. Cerati,[56] A. Cervelli,[73] A. Cervera Villanueva,[72] M. Chalifour,[18] C. Chang,[25] E. Chardonnet,[1] A. Chatterjee,[136] S. Chattopadhyay,[163] J. Chaves,[132] H. Chen,[15] M. Chen,[23] Y. Chen,[10] D. Cherdack,[69] C. Chi,[39] S. Childress,[56] A. Chiriacescu,[16] K. Cho,[97] S. Choubey,[66] A. Christensen,[38] D. Christian,[56] G. Christodoulou,[18] E. Church,[130] P. Clarke,[50] T. E. Coan,[150] A. G. Cocco,[78] J. A. B. Coelho,[102] E. Conley,[46] J. M. Conrad,[115] M. Convery,[143] L. Corwin,[147] P. Cotte,[17] L. Cremaldi,[119] L. Cremonesi,[161] J. I. Crespo-Anadón,[39] E. Cristaldo,[6] R. Cross,[107] C. Cuesta,[19] Y. Cui,[25] D. Cussans,[14] M. Dabrowski,[15] H. da Motta,[30] L. Da Silva Peres,[55] Q. David,[81] G. S. Davies,[119] S. Davini,[75] J. Dawson,[1] K. De,[157] R. M. De Almeida,[58] P. Debbins,[90] I. De Bonis,[20] M. P. Decowski,[122] A. de Gouvêa,[125] P. C. De Holanda,[29] I. L. De Icaza Astiz,[153] A. Deisting,[85] P. De Jong,[122] A. Delbart,[17] D. Delepine,[64] M. Delgado,[3] A. Dell'Acqua,[18] P. De Lurgio,[4] J. R. T. de Mello Neto,[55] D. M. DeMuth,[162] S. Dennis,[109] C. Densham,[142] G. Deptuch,[56] A. De Roeck,[18] V. De Romeri,[72] J. J. De Vries,[28] R. Dharmapalan,[68] F. Diaz,[137] J. S. Díaz,[88] S. Di Domizio,[75] L. Di Giulio,[18] P. Ding,[56] L. Di Noto,[75] C. Distefano,[152] R. Diurba,[160] M. Diwan,[15] Z. Djurcic,[4] N. Dokania,[151] M. J. Dolinski,[45] L. Domine,[143] D. Douglas,[117] F. Drielsma,[143] D. Duchesneau,[20] K. Duffy,[56] P. Dunne,[85] T. Durkin,[142] H. Duyang,[149] O. Dvornikov,[68] D. A. Dwyer,[108] A. S. Dyshkant,[124] M. Eads,[124] D. Edmunds,[117] J. Eisch,[91] S. Emery,[17] A. Ereditato,[10] C. O. Escobar,[56] L. Escudero Sanchez,[28] J. J. Evans,[114] K. Ewart,[88] A. C. Ezeribe,[146] K. Fahey,[56] A. Falcone,[76] C. Farnese,[131] Y. Farzan,[82] J. Felix,[64] E. Fernandez-Martinez,[113] P. Fernandez Menendez,[72] F. Ferraro,[75] L. Fields,[56] A. Filkins,[168] F. Filthaut,[122] R. S. Fitzpatrick,[116] W. Flanagan,[43] B. Fleming,[170] R. Flight,[140] J. Fowler,[46] W. Fox,[88] J. Franc,[41] K. Francis,[124] D. Franco,[170] J. Freeman,[56] J. Freestone,[114] J. Fried,[15] A. Friedland,[143] S. Fuess,[56] I. Furic,[57] A. P. Furmanski,[160] A. Gago,[137] H. Gallagher,[159] A. Gallego-Ros,[19] N. Gallice,[77, 76] V. Galymov,[81] E. Gamberini,[18] T. Gamble,[146] R. Gandhi,[66] R. Gandrajula,[117] S. Gao,[15] D. Garcia-Gamez,[62] M. Á. García-Peris,[72] S. Gardiner,[56] D. Gastler,[13] G. Ge,[39] B. Gelli,[29] A. Gendotti,[49] S. Gent,[148] Z. Ghorbani-Moghaddam,[75] D. Gibin,[131] I. Gil-Botella,[19] C. Girerd,[81] A. K. Giri,[87] D. Gnani,[108] O. Gogota,[101] M. Gold,[120] S. Gollapinni,[110] K. Gollwitzer,[56] R. A. Gomes,[52] L. V. Gomez Bermeo,[145] L. S. Gomez Fajardo,[145] F. Gonnella,[12] J. A. Gonzalez-Cuevas,[6] M. C. Goodman,[4] O. Goodwin,[114] S. Goswami,[134] C. Gotti,[76] E. Goudzovski,[12] C. Grace,[108] M. Graham,[143] E. Gramellini,[170] R. Gran,[118] E. Granados,[64] A. Grant,[44] C. Grant,[13] D. Gratieri,[58] P. Green,[114] S. Green,[28] L. Greenler,[169] M. Greenwood,[128] J. Greer,[14] W. C. Griffith,[153] M. Groh,[88] J. Grudzinski,[4] K. Grzelak,[165] W. Gu,[15] V. Guarino,[4] R. Guenette,[67] A. Guglielmi,[131] B. Guo,[149] K. K. Guthikonda,[65] R. Gutierrez,[3] P. Guzowski,[114] M. M. Guzzo,[29] S. Gwon,[33] A. Habig,[118] A. Hackenburg,[170] H. Hadavand,[157] R. Haenni,[10] A. Hahn,[56] J. Haigh,[166] J. Haiston,[147] T. Hamernik,[56] P. Hamilton,[85] J. Han,[136] K. Harder,[142] D. A. Harris,[172, 56] J. Hartnell,[153] T. Hasegawa,[96] R. Hatcher,[56] E. Hazen,[13] A. Heavey,[56] K. M. Heeger,[170] K. Hennessy,[109] S. Henry,[140] M. A. Hernandez Morquecho,[64] K. Herner,[56] L. Hertel,[23] A. S. Hesam,[18] J. Hewes,[34] A. Higuera,[69] T. Hill,[83] S. J. Hillier,[12] A. Himmel,[56] J. Hoff,[56] C. Hohl,[9] A. Holin,[161] E. Hoppe,[130] G. A. Horton-Smith,[98] M. Hostert,[47] A. Hourlier,[115] B. Howard,[88] R. Howell,[140] J. Huang,[158] J. Huang,[22] J. Hugon,[111] G. Iles,[85] A. M. Iliescu,[73] R. Illingworth,[56] A. Ioannisian,[171] R. Itay,[143]

A. Izmaylov,[72] E. James,[56] B. Jargowsky,[23] F. Jediny,[41] C. Jesús-Valls,[71] X. Ji,[15] L. Jiang,[164] S. Jiménez,[19] A. Jipa,[16] A. Joglekar,[25] C. Johnson,[38] R. Johnson,[34] B. Jones,[157] S. Jones,[161] C. K. Jung,[151] T. Junk,[56] Y. Jwa,[39] M. Kabirnezhad,[129] A. Kaboth,[142] I. Kadenko,[101] F. Kamiya,[54] G. Karagiorgi,[39] A. Karcher,[108] M. Karolak,[17] Y. Karyotakis,[20] S. Kasai,[100] S. P. Kasetti,[111] L. Kashur,[38] N. Kazaryan,[171] E. Kearns,[13] P. Keener,[132] K.J. Kelly,[56] E. Kemp,[29] W. Ketchum,[56] S. H. Kettell,[15] M. Khabibullin,[80] A. Khotjantsev,[80] A. Khvedelidze,[59] D. Kim,[18] B. King,[56] B. Kirby,[15] M. Kirby,[56] J. Klein,[132] K. Koehler,[169] L. W. Koerner,[69] S. Kohn,[21,108] P. P. Koller,[10] M. Kordosky,[168] T. Kosc,[81] U. Kose,[18] V. A. Kostelecký,[88] K. Kothekar,[14] F. Krennrich,[91] I. Kreslo,[10] Y. Kudenko,[80] V. A. Kudryavtsev,[146] S. Kulagin,[80] J. Kumar,[68] R. Kumar,[139] C. Kuruppu,[149] V. Kus,[41] T. Kutter,[111] A. Lambert,[108] K. Lande,[132] C. E. Lane,[45] K. Lang,[158] T. Langford,[170] P. Lasorak,[153] D. Last,[132] C. Lastoria,[19] A. Laundrie,[169] A. Lawrence,[108] I. Lazanu,[16] R. LaZur,[38] T. Le,[159] J. Learned,[68] P. LeBrun,[81] G. Lehmann Miotto,[18] R. Lehnert,[88] M. A. Leigui de Oliveira,[54] M. Leitner,[108] M. Leyton,[71] L. Li,[23] S. Li,[15] S. W. Li,[143] T. Li,[50] Y. Li,[15] H. Liao,[98] C. S. Lin,[108] S. Lin,[38] A. Lister,[169] B. R. Littlejohn,[84] J. Liu,[23] S. Lockwitz,[56] T. Loew,[108] M. Lokajicek,[40] I. Lomidze,[59] K. Long,[85] K. Loo,[95] D. Lorca,[10] T. Lord,[166] J. M. LoSecco,[126] W. C. Louis,[110] K.B. Luk,[21,108] X. Luo,[26] N. Lurkin,[12] T. Lux,[71] V. P. Luzio,[54] D. MacFarland,[143] A. A. Machado,[29] P. Machado,[56] C. T. Macias,[88] J. R. Macier,[56] A. Maddalena,[61] P. Madigan,[21,108] S. Magill,[4] K. Mahn,[117] A. Maio,[103,106] J. A. Maloney,[42] G. Mandrioli,[73] J. C. Maneira,[103,106] L. Manenti,[161] S. Manly,[140] A. Mann,[159] K. Manolopoulos,[142] M. Manrique Plata,[88] A. Marchionni,[56] W. Marciano,[15] D. Marfatia,[68] C. Mariani,[164] J. Maricic,[68] F. Marinho,[53] A. D. Marino,[37] M. Marshak,[160] C. Marshall,[108] J. Marshall,[166] J. Marteau,[81] J. Martin-Albo,[72] N. Martinez,[138] D.A. Martinez Caicedo,[147] S. Martynenko,[151] K. Mason,[159] A. T. Mastbaum,[141] M. Masud,[72] S. Matsuno,[68] J. Matthews,[111] C. Mauger,[132] N. Mauri,[73] K. Mavrokoridis,[109] R. Mazza,[76] A. Mazzacane,[56] E. Mazzucato,[17] E. McCluskey,[56] N. McConkey,[114] K. S. McFarland,[140] C. McGrew,[151] A. McNab,[114] A. Mefodiev,[80] P. Mehta,[94] P. Melas,[7] M. Mellinato,[76] O. Mena,[72] S. Menary,[172] L. Mendes Santos,[29] H. Mendez,[138] A. Menegolli,[79] G. Meng,[131] M. D. Messier,[88] W. Metcalf,[111] M. Mewes,[88] H. Meyer,[167] T. Miao,[56] G. Michna,[148] T. Miedema,[122] J. Migenda,[146] R. Milincic,[68] W. Miller,[160] J. Mills,[159] C. Milne,[83] O. Mineev,[80] O. G. Miranda,[35] S. Miryala,[15] C. S. Mishra,[56] S. R. Mishra,[149] A. Mislivec,[160] D. Mladenov,[18] I. Mocioiu,[133] K. Moffat,[47] N. Moggi,[73] R. Mohanta,[70] T. A. Mohayai,[56] N. Mokhov,[56] J. Molina,[6] L. Molina Bueno,[49] A. Montanari,[73] C. Montanari,[79] D. Montanari,[56] L. M. Montano Zetina,[35] J. Moon,[115] M. Mooney,[38] A. Moor,[28] D. Moreno,[3] B. Morgan,[166] C. Morris,[69] C. Mossey,[56] E. Motuk,[161] C. A. Moura,[54] J. Mousseau,[116] W. Mu,[56] L. Mualem,[27] J. Mueller,[38] M. Muether,[167] S. Mufson,[88] F. Muheim,[50] A. Muir,[44] M. Mulhearn,[22] H. Muramatsu,[160] S. Murphy,[49] J. Musser,[88] J. Nachtman,[90] S. Nagu,[112] M. Nalbandyan,[171] R. Nandakumar,[142] D. Naples,[136] S. Narita,[92] D. Navas-Nicolás,[19] N. Nayak,[23] M. Nebot-Guinot,[50] L. Necib,[27] K. Negishi,[92] J. K. Nelson,[168] J. Nesbit,[169] M. Nessi,[18] D. Newbold,[142] M. Newcomer,[132] D. Newhart,[56] R. Nichol,[161] E. Niner,[56] K. Nishimura,[68] A. Norman,[56] R. Northrop,[32] P. Novella,[72] J. A. Nowak,[107] M. Oberling,[4] A. Olivares Del Campo,[47] A. Olivier,[140] Y. Onel,[90] Y. Onishchuk,[101] J. Ott,[23] L. Pagani,[22] S. Pakvasa,[68] O. Palamara,[56] S. Palestini,[18] J. M. Paley,[56] M. Pallavicini,[75] C. Palomares,[19] E. Pantic,[22] V. Paolone,[136] V. Papadimitriou,[56] R. Papaleo,[152] A. Papanestis,[142] S. Paramesvaran,[14] S. Parke,[56] Z. Parsa,[15] M. Parvu,[16] S. Pascoli,[47] L. Pasqualini,[73] J. Pasternak,[85] J. Pater,[114] C. Patrick,[161] L. Patrizii,[73] R. B. Patterson,[27] S. J. Patton,[108] T. Patzak,[1] A. Paudel,[98] B. Paulos,[169] L. Paulucci,[54] Z. Pavlovic,[56] G. Pawloski,[160] D. Payne,[109] V. Pec,[146] S. J. M. Peeters,[153] Y. Penichot,[17] E. Pennacchio,[81] A. Penzo,[90] O. L. G. Peres,[29] J. Perry,[50] D. Pershey,[46] G. Pessina,[76] G. Petrillo,[143] C. Petta,[74] R. Petti,[149] F. Piastra,[10] L. Pickering,[117] F. Pietropaolo,[18,131] J. Pillow,[166] R. Plunkett,[56] R. Poling,[160] X. Pons,[18] N. Poonthottathil,[91] S. Pordes,[56] M. Potekhin,[15] R. Potenza,[74] B. V. K. S. Potukuchi,[93] J. Pozimski,[85] M. Pozzato,[73] S. Prakash,[29] T. Prakash,[108] S. Prince,[67] D. Pugnere,[81] K. Qi,[151] X. Qian,[15] J. L. Raaf,[56] R. Raboanary,[2] V. Radeka,[15] J. Rademacker,[14] B. Radics,[49] A. Rafique,[4] E. Raguzin,[15] M. Rai,[166] M. Rajaoalisoa,[34] I. Rakhno,[56] H. T. Rakotondramanana,[2] L. Rakotondravohitra,[2] Y. A. Ramachers,[166] R. Rameika,[56] M. A. Ramirez Delgado,[64] B. Ramson,[56] A. Rappoldi,[79] G. Raselli,[79] P. Ratoff,[107] S. Ravat,[18] H. Razafinime,[2] J.S. Real,[63] B. Rebel,[169,56] D. Redondo,[19] M. Reggiani-Guzzo,[29] T. Rehak,[45] J. Reichenbacher,[147] S. D. Reitzner,[56] A. Renshaw,[69] S. Rescia,[15] F. Resnati,[18] A. Reynolds,[129] G. Riccobene,[152] L. C. J. Rice,[136] K. Rielage,[110] Y. Rigaut,[49] D. Rivera,[132] L. Rochester,[143] M. Roda,[109] P. Rodrigues,[129] M. J. Rodriguez Alonso,[18] J. Rodriguez Rondon,[147] A. J. Roeth,[46] H. Rogers,[38] S. Rosauro-Alcaraz,[113] M. Rossella,[79] J. Rout,[94] S. Roy,[66] A. Rubbia,[49] C. Rubbia,[60] B. Russell,[108] J. Russell,[143] D. Ruterbories,[140] R. Saakyan,[161] S. Sacerdoti,[1] T. Safford,[117] N. Sahu,[87] P. Sala,[77,18] N. Samios,[15] M. C. Sanchez,[91] D. A. Sanders,[119] D. Sankey,[142] S. Santana,[138] M. Santos-Maldonado,[138] N. Saoulidou,[7] P. Sapienza,[152] C. Sarasty,[34] I. Sarcevic,[5] G. Savage,[56] V. Savinov,[136] A. Scaramelli,[79] A. Scarff,[146] A. Scarpelli,[1]

T. Schaffer,[118] H. Schellman,[128,56] P. Schlabach,[56] D. Schmitz,[32] K. Scholberg,[46] A. Schukraft,[56] E. Segreto,[29] J. Sensenig,[132] I. Seong,[23] A. Sergi,[12] F. Sergiampietri,[151] D. Sgalaberna,[18] M. H. Shaevitz,[39] S. Shafaq,[94] M. Shamma,[25] H. R. Sharma,[93] R. Sharma,[15] T. Shaw,[56] C. Shepherd-Themistocleous,[142] S. Shin,[32] D. Shooltz,[117] R. Shrock,[151] L. Simard,[102] N. Simos,[15] J. Sinclair,[10] G. Sinev,[46] J. Singh,[112] J. Singh,[112] R. Sipos,[18] F. W. Sippach,[39] G. Sirri,[73] A. Sitraka,[147] K. Siyeon,[33] D. Smargianaki,[151] A. Smith,[46] A. Smith,[28] E. Smith,[88] P. Smith,[88] J. Smolik,[41] M. Smy,[23] P. Snopok,[84] M. Soares Nunes,[29] H. Sobel,[23] M. Soderberg,[154] C. J. Solano Salinas,[89] S. Söldner-Rembold,[114] N. Solomey,[167] V. Solovov,[104] W. E. Sondheim,[110] M. Sorel,[72] J. Soto-Oton,[19] A. Sousa,[34] K. Soustruznik,[31] F. Spagliardi,[129] M. Spanu,[15] J. Spitz,[116] N. J. Spooner,[146] K. Spurgeon,[154] R. Staley,[12] M. Stancari,[56] L. Stanco,[131] H. M. Steiner,[108] J. Stewart,[15] B. Stillwell,[32] J. Stock,[147] F. Stocker,[18] T. Stokes,[111] M. Strait,[160] T. Strauss,[56] S. Striganov,[56] A. Stuart,[36] D. Summers,[119] A. Surdo,[144] V. Susic,[9] L. Suter,[56] C. M. Sutera,[74] R. Svoboda,[22] B. Szczerbinska,[156] A. Szelc,[114] R. Talaga,[4] H. A. Tanaka,[143] B. Tapia Oregui,[158] A. Tapper,[85] S. Tariq,[56] E. Tatar,[83] R. Tayloe,[88] A. M. Teklu,[151] M. Tenti,[73] K. Terao,[143] C. A. Ternes,[72] F. Terranova,[76] G. Testera,[75] A. Thea,[142] J. L. Thompson,[146] C. Thorn,[15] S. C. Timm,[56] A. Tonazzo,[1] M. Torti,[76] M. Tortola,[72] F. Tortorici,[74] D. Totani,[56] M. Toups,[56] C. Touramanis,[109] J. Trevor,[27] W. H. Trzaska,[95] Y. T. Tsai,[143] Z. Tsamalaidze,[59] K. V. Tsang,[143] N. Tsverava,[59] S. Tufanli,[18] C. Tull,[108] E. Tyley,[146] M. Tzanov,[111] M. A. Uchida,[28] J. Urheim,[88] T. Usher,[143] M. R. Vagins,[99] P. Vahle,[168] G. A. Valdiviesso,[51] E. Valencia,[168] Z. Vallari,[27] J. W. F. Valle,[72] S. Vallecorsa,[18] R. Van Berg,[132] R. G. Van de Water,[110] D. Vanegas Forero,[29] F. Varanini,[131] D. Vargas,[71] G. Varner,[68] J. Vasel,[88] G. Vasseur,[17] K. Vaziri,[56] S. Ventura,[131] A. Verdugo,[19] S. Vergani,[28] M. A. Vermeulen,[122] M. Verzocchi,[56] H. Vieira de Souza,[29] C. Vignoli,[61] C. Vilela,[151] B. Viren,[15] T. Vrba,[41] T. Wachala,[121] A. V. Waldron,[85] M. Wallbank,[34] H. Wang,[24] J. Wang,[22] Y. Wang,[24] Y. Wang,[151] K. Warburton,[91] D. Warner,[38] M. Wascko,[85] D. Waters,[161] A. Watson,[12] P. Weatherly,[45] A. Weber,[142,129] M. Weber,[10] H. Wei,[15] A. Weinstein,[91] D. Wenman,[169] M. Wetstein,[91] M. R. While,[147] A. White,[157] L. H. Whitehead,[28] D. Whittington,[154] M. J. Wilking,[151] C. Wilkinson,[10] Z. Williams,[157] F. Wilson,[142] R. J. Wilson,[38] J. Wolcott,[159] T. Wongjirad,[159] K. Wood,[151] L. Wood,[130] E. Worcester,[15] M. Worcester,[15] C. Wret,[140] W. Wu,[56] W. Wu,[23] Y. Xiao,[23] G. Yang,[151] T. Yang,[56] N. Yershov,[80] K. Yonehara,[56] T. Young,[123] B. Yu,[15] J. Yu,[157] J. Zalesak,[40] L. Zambelli,[20] B. Zamorano,[62] A. Zani,[77] L. Zazueta,[168] G. P. Zeller,[56] J. Zennamo,[56] K. Zeug,[169] C. Zhang,[15] M. Zhao,[15] E. Zhivun,[15] G. Zhu,[127] E. D. Zimmerman,[37] M. Zito,[17] S. Zucchelli,[73] J. Zuklin,[40] V. Zutshi,[124] and R. Zwaska[56]

(The DUNE Collaboration)

[1] *APC - Université de Paris, CNRS/IN2P3, CEA/lrfu, Observatoire de Paris, 10, rue Alice Domon et Léonie Duquet, 75205 Paris Cedex 13, France*
[2] *University of Antananarivo, BP 566, Antananarivo 101, Madagascar*
[3] *Universidad Antonio Nariño, Cra 3 Este No 47A-15, Bogotá, Colombia*
[4] *Argonne National Laboratory, Argonne, IL 60439, USA*
[5] *University of Arizona, 1118 E. Fourth Street Tucson, AZ 85721, USA*
[6] *Universidad Nacional de Asunción, San Lorenzo, Paraguay*
[7] *University of Athens, University Campus, Zografou GR 157 84, Greece*
[8] *Universidad del Atlantico, Carrera 30 Número 8- 49 Puerto Colombia - Atlántico, Colombia*
[9] *University of Basel, Klingelbergstrasse 82, CH-4056 Basel, Switzerland*
[10] *University of Bern, Sidlerstrasse 5, CH-3012 Bern, Switzerland*
[11] *Beykent University, Istanbul*
[12] *University of Birmingham, Edgbaston, Birmingham B15 2TT, United Kingdom*
[13] *Boston University, Boston, MA 02215, USA*
[14] *University of Bristol, H. H. Wills Physics Laboratory, Tyndall Avenue Bristol BS8 1TL, United Kingdom*
[15] *Brookhaven National Laboratory, Upton, NY 11973, USA*
[16] *University of Bucharest, Faculty of Physics, Bucharest, Romania*
[17] *CEA/Saclay, IRFU Institut de Recherche sur les Lois Fondamentales de l'Univers, F-91191 Gif-sur-Yvette CEDEX, France*
[18] *CERN, European Organization for Nuclear Research 1211 Genève 23, Switzerland, CERN*
[19] *CIEMAT, Centro de Investigaciones Energéticas, Medioambientales y Tecnológicas, Av. Complutense, 40, E-28040 Madrid, Spain*
[20] *Laboratoire d'Annecy-le-Vieux de Physique des Particules, CNRS/IN2P3 and Université Savoie Mont Blanc, CNRS/IN2P3 and Université Savoie Mont Blanc, 74941 Annecy-le-Vieux, France*
[21] *University of California Berkeley, Berkeley, CA 94720, USA*
[22] *University of California Davis, Davis, CA 95616, USA*
[23] *University of California Irvine, Irvine, CA 92697, USA*
[24] *University of California Los Angeles, Los Angeles, CA 90095, USA*
[25] *University of California Riverside, 900 University Ave, Riverside CA 92521*
[26] *University of California Santa Barbara, Santa Barbara, California 93106 USA*

[27]California Institute of Technology, Pasadena, CA 91125, USA
[28]University of Cambridge, JJ Thomson Avenue, Cambridge CB3 0HE, United Kingdom
[29]Universidade Estadual de Campinas, Campinas - SP, 13083-970, Brazil
[30]Centro Brasileiro de Pesquisas Físicas, Rio de Janeiro, RJ 22290-180, Brazil
[31]Institute of Particle and Nuclear Physics of the Faculty of Mathematics and Physics of the Charles University in Prague, V Holešovičkách 747/2, 180 00 Praha 8-Libeň, Czech Republic
[32]University of Chicago, Chicago, IL 60637, USA
[33]Chung-Ang University, Dongjak-Gu, Seoul 06974, South Korea
[34]University of Cincinnati, Cincinnati, OH 45221, USA
[35]Centro de Investigacion y de Estudios Avanzados del IPN (Cinvestav), Mexico City
[36]Universidad de Colima, 340 Colonia Villa San Sebastian Colima, Colima, Mexico
[37]University of Colorado Boulder, Boulder, CO 80309, USA
[38]Colorado State University, Fort Collins, CO 80523, USA
[39]Columbia University, New York, NY 10027, USA
[40]Institute of Physics, Czech Academy of Sciences, Na Slovance 2, 182 21 Praha 8, Czech Republic
[41]Czech Technical University in Prague, Břehová 78/7, 115 19 Prague 1, Czech Republic
[42]Dakota State University, Madison, SD 57042, USA
[43]University of Dallas, Irving, TX 75062-4736, USA
[44]Daresbury Laboratory, Daresbury Warrington, Cheshire WA4 4AD, United Kingdom
[45]Drexel University, Philadelphia, PA 19104, USA
[46]Duke University, Durham, NC 27708, USA
[47]Durham University, South Road, Durham DH1 3LE, United Kingdom
[48]Universidad EIA, Via José María Córdoba #km 2 + 200, Envigado, Antioquia
[49]ETH Zurich, Institute for Particle Physics, Zurich, Switzerland
[50]University of Edinburgh, Edinburgh EH8 9YL, United Kingdom
[51]Universidade Federal de Alfenas, Poços de Caldas - MG, 37715-400, Brazil
[52]Universidade Federal de Goias, Goiania, GO 74690-900, Brazil
[53]Universidade Federal de São Carlos, Araras - SP, 13604-900, Brazil
[54]Universidade Federal do ABC, Av. dos Estados 5001, Santo André - SP, 09210-580 Brazil
[55]Universidade Federal do Rio de Janeiro, Rio de Janeiro - RJ, 21941-901, Brazil
[56]Fermi National Accelerator Laboratory, Batavia, IL 60510
[57]University of Florida, PO Box 118440 Gainesville, FL 32611-8440, USA
[58]Fluminense Federal University, Rua Miguel de Frias, 9 Icaraí Niterói - RJ, 24220-900, Brazil
[59]Georgian Technical University, 77 Kostava Str. 0160, Tbilisi, Georgia
[60]Gran Sasso Science Institute, Viale Francesco Crispi 7, L'Aquila, Italy
[61]Laboratori Nazionali del Gran Sasso, I-67010 Assergi, AQ, Italy
[62]University of Granada & CAFPE, Campus Fuentenueva (Edif. Mecenas), 18002 Granada, Spain
[63]University Grenoble Alpes, CNRS, Grenoble INP, LPSC-IN2P3, 38000 Grenoble, France
[64]Universidad de Guanajuato, Gto., C.P. 37000, Mexico
[65]Department of Physics, K L E F, Green Fields, Guntur - 522 502, AP, India
[66]Harish-Chandra Research Institute, Jhunsi, Allahabad 211 019, India
[67]Harvard University, 17 Oxford St. Cambridge, MA 02138, USA
[68]University of Hawaii, Honolulu, HI 96822, USA
[69]University of Houston, Houston, TX 77204, USA
[70]University of Hyderabad, Gachibowli, Hyderabad - 500 046, India
[71]Institut de Fìsica d'Altes Energies, Barcelona i.e. Catalan ersitat Autonoma de Barcelona, Campus UAB, Facultat Ciències Nord, 08193 Bellaterra, Barcelona, Spain
[72]Instituto de Fisica Corpuscular, Catedratico Jose Beltran, 2 E-46980 Paterna (Valencia), Spain
[73]Istituto Nazionale di Fisica Nucleare Bologna, 40127 Bologna BO, Italy
[74]Istituto Nazionale di Fisica Nucleare Sezione di Catania, Via Santa Sofia 64, I-95123 Catania, Italy
[75]Università degli studi di Genova, Istituto Nazionale di Fisica Nucleare Genova, 16126 Genova GE, Italy
[76]Istituto Nazionale di Fisica Nucleare Sezione di Milano Bicocca and University of Milano Bicocca, Piazza della Scienza, 3 - I-20126 Milano, Italy
[77]Istituto Nazionale di Fisica Nucleare Milano, I-20133 Milano, Italy
[78]Istituto Nazionale di Fisica Nucleare - Sezione di Napoli, Complesso Universitario di Monte S. Angelo, I-80126 Napoli, Italy
[79]Università degli studi di Pavia, Istituto Nazionale di Fisica Nucleare Sezione di Pavia, I-27100 Pavia, Italy
[80]Institute for Nuclear Research of the Russian Academy of Sciences , prospekt 60-letiya Oktyabrya 7a, Moscow 117312, Russia
[81]Institut de Physique des 2 Infinis de Lyon, Rue E. Fermi 4 69622 Villeurbanne, France
[82]Institute for Research in Fundamental Sciences , Farmanieh St. Tehran, 19538-33511, Iran
[83]Idaho State University, Department of Physics, Pocatello, ID 83209, USA
[84]Illinois Institute of Technology, Chicago, IL 60616, USA
[85]Imperial College of Science Technology and Medicine, Blackett Laboratory Prince Consort Road, London SW7 2BZ, United Kingdom
[86]Indian Institute of Technology Guwahati, Guwahati, 781 039, India

[87]*Indian Institute of Technology Hyderabad, Hyderabad, 502285, India*
[88]*Indiana University, Bloomington, IN 47405, USA*
[89]*Universidad Nacional de Ingeniería, Av. Tupac Amaru 210, Lima 25, Perú*
[90]*University of Iowa, Department of Physics and Astronomy 203 Van Allen Hall Iowa City, IA 52242, USA*
[91]*Iowa State University, Ames, Iowa 50011, USA*
[92]*Iwate University, Morioka, Iwate 020-8551, Japan*
[93]*University of Jammu, Physics Department, JAMMU-180006, India*
[94]*Jawaharlal Nehru University, School of Physical Sciences, New Delhi 110067, India*
[95]*University of Jyvaskyla, P.O. Box 35, FI-40014, Finland*
[96]*High Energy Accelerator Research Organization (KEK), Ibaraki, 305-0801, Japan*
[97]*Korea Institute of Science and Technology Information, Daejeon, 34141, South Korea*
[98]*Kansas State University, Manhattan, KS 66506, USA*
[99]*Kavli Institute for the Physics and Mathematics of the Universe , Kashiwa, Chiba 277-8583, Japan*
[100]*National Institute of Technology, Kure College, Hiroshima, 737-8506, Japan*
[101]*Kyiv National University, 64, 01601 Kyiv, Ukraine*
[102]*Laboratoire de l'Accélérateur Linéaire , Bâtiment 200, 91440 Orsay, France*
[103]*Laboratório de Instrumentação e Física Experimental de Partículas - LIP, Lisboa, Portugal*
[104]*Laboratório de Instrumentação e Física Experimental de Partículas - LIP, Coimbra, Portugal*
[105]*Instituto Superior Técnico - IST, Universidade de Lisboa, Portugal*
[106]*Faculdade de Ciências - FCUL, Universidade de Lisboa, Portugal*
[107]*Lancaster University, Bailrigg, Lancaster LA1 4YB, United Kingdom*
[108]*Lawrence Berkeley National Laboratory, Berkeley, CA 94720, USA*
[109]*University of Liverpool, L69 7ZE, Liverpool, United Kingdom*
[110]*Los Alamos National Laboratory, Los Alamos, NM 87545, USA*
[111]*Louisiana State University, Baton Rouge, LA 70803, USA*
[112]*University of Lucknow, Lucknow 226007, Uttar Pradesh, India*
[113]*Madrid Autonoma University and IFT UAM/CSIC, Ciudad Universitaria de Cantoblanco 28049 Madrid, Spain*
[114]*University of Manchester, Oxford Road, Manchester M13 9PL, United Kingdom*
[115]*Massachusetts Institute of Technology, Cambridge, MA 02139, USA*
[116]*University of Michigan, Ann Arbor, MI 48109, USA*
[117]*Michigan State University, East Lansing, MI 48824, USA*
[118]*University of Minnesota Duluth, Duluth, MN 55812, USA*
[119]*University of Mississippi, P.O. Box 1848, University, MS 38677 USA*
[120]*University of New Mexico, 1919 Lomas Blvd. N.E. Albuquerque, NM 87131, USA*
[121]*H. Niewodniczański Institute of Nuclear Physics, Polish Academy of Sciences, Cracow, Poland*
[122]*Nikhef National Institute of Subatomic Physics, Science Park, Amsterdam, Netherlands*
[123]*University of North Dakota, 3501 University Ave Grand Forks, ND 58202-8357, USA*
[124]*Northern Illinois University, Department of Physics, DeKalb, Illinois 60115, USA*
[125]*Northwestern University, Evanston, Il 60208, USA*
[126]*University of Notre Dame, Notre Dame, IN 46556, USA*
[127]*Ohio State University, 191 W. Woodruff Ave. Columbus, OH 43210, USA*
[128]*Oregon State University, Corvallis, OR 97331, USA*
[129]*University of Oxford, Oxford, OX1 3RH, United Kingdom*
[130]*Pacific Northwest National Laboratory, Richland, WA 99352, USA*
[131]*Universtà Degli Studi di Padova, Dip. Fisica e Astronomia G. Galilei and INFN Sezione di Padova, I-35131 Padova, Italy*
[132]*University of Pennsylvania, Philadelphia, PA 19104, USA*
[133]*Pennsylvania State University, University Park, PA 16802, USA*
[134]*Physical Research Laboratory, Ahmedabad 380 009, India*
[135]*Università di Pisa, Theor. Division; Largo B. Pontecorvo 3, Ed. B-C, I-56127 Pisa, Italy*
[136]*University of Pittsburgh, Pittsburgh, PA 15260, USA*
[137]*Pontificia Universidad Católica del Perú, Apartado 1761, Lima, Perú*
[138]*University of Puerto Rico, Mayaguez, 00681, USA*
[139]*Punjab Agricultural University, Department of Math. Stat. & Physics, Ludhiana 141004, India*
[140]*University of Rochester, Rochester, NY 14627, USA*
[141]*Rutgers University, Piscataway, NJ, 08854, USA*
[142]*STFC Rutherford Appleton Laboratory, OX11 0QX Harwell Campus, Didcot, United Kingdom*
[143]*SLAC National Acceleratory Laboratory, Menlo Park, CA 94025, USA*
[144]*Università del Salento and Istituto Nazionale Fisica Nucleare, Via Provinciale per Arnesano, 73100 Lecce, Italy*
[145]*Universidad Sergio Arboleda, Cll 74 -14 -14, 11022 Bogotá, Colombia*
[146]*University of Sheffield, Department of Physics and Astronomy, Sheffield S3 7RH, United Kingdom*
[147]*South Dakota School of Mines and Technology, Rapid City, SD 57701, USA*
[148]*South Dakota State University, Brookings, SD 57007, USA*
[149]*University of South Carolina, Columbia, SC 29208, USA*
[150]*Southern Methodist University, Dallas, TX 75275, USA*

[151] *Stony Brook University, SUNY, Stony Brook, New York 11794, USA*
[152] *INFN - Laboratori Nazionali del Sud (LNS), Via S. Sofia 62, 95123 Catania, Italy*
[153] *University of Sussex, Brighton, BN1 9RH, United Kingdom*
[154] *Syracuse University, Syracuse, NY 13244, USA*
[155] *University of Tennessee at Knoxville, TN, 37996, USA*
[156] *Texas A&M University (Corpus Christi), Corpus Christi, TX 78412, USA*
[157] *University of Texas at Arlington, Arlington, TX 76019, USA*
[158] *University of Texas at Austin, Austin, TX 78712, USA*
[159] *Tufts University, Medford, MA 02155, USA*
[160] *University of Minnesota Twin Cities, Minneapolis, MN 55455, USA*
[161] *University College London, London, WC1E 6BT, United Kingdom*
[162] *Valley City State University, Valley City, ND 58072, USA*
[163] *Variable Energy Cyclotron Centre, 1/AF, Bidhannagar Kolkata - 700 064 West Bengal, India*
[164] *Virginia Tech, Blacksburg, VA 24060, USA*
[165] *University of Warsaw, Faculty of Physics ul. Pasteura 5 02-093 Warsaw, Poland*
[166] *University of Warwick, Coventry CV4 7AL, United Kingdom*
[167] *Wichita State University, Physics Division, Wichita, KS 67260, USA*
[168] *William and Mary, Williamsburg, VA 23187, USA*
[169] *University of Wisconsin Madison, Madison, WI 53706, USA*
[170] *Yale University, New Haven, CT 06520, USA*
[171] *Yerevan Institute for Theoretical Physics and Modeling, Halabian Str. 34, Yerevan 0036, Armenia*
[172] *York University, Physics and Astronomy Department, 4700 Keele St. Toronto M3J 1P3, Canada*

Contents

Contents i

List of Figures ii

List of Tables 1

A Roadmap of the DUNE Technical Design Report 1

1 DUNE Physics 2
- 1.1 Goals of the DUNE Science Program . . . 2
  - 1.1.1 Neutrino Oscillations: Masses, Mixing Angles and CP Violation . . . 2
  - 1.1.2 Baryon Number Violation . . . 6
  - 1.1.3 Supernova Neutrino Bursts . . . 6
  - 1.1.4 Additional Beyond-Standard-Model Physics Signatures . . . 8
- 1.2 Summary of Assumptions and Methods Employed . . . 11
  - 1.2.1 Beam and Detector . . . 11
  - 1.2.2 Deployment Scenario . . . 12
  - 1.2.3 Simulation, Reconstruction, and Data Analysis Tools . . . 12
- 1.3 Selected Results from Sensitivity Studies . . . 13
  - 1.3.1 CPV in the Neutrino Sector and Precise Oscillation Parameter Measurements . . . 13
  - 1.3.2 Proton Decay and Other Baryon-number Violating Processes . . . 24
  - 1.3.3 Galactic Supernovae via Measurements of Neutrino Bursts . . . 25
  - 1.3.4 Searches for Beyond-Standard-Model Physics . . . 26

Glossary 30

References 34

List of Figures

1.1 Appearance probabilities for ν_e and $\bar{\nu}_e$ at 1300 km 5
1.2 Summary of nucleon decay experimental limits and model predictions 7
1.3 Expected time-dependent neutrino burst characteristics for a core-collapse supernova . . 9
1.4 ν_e and $\bar{\nu}_e$ appearance spectra 15
1.5 ν_μ and $\bar{\nu}_\mu$ disappearance spectra 17
1.6 Significance of the DUNE determination of CP violation 18
1.7 Significance of the DUNE neutrino mass ordering determination, as a function of time . 19
1.8 Resolution for the DUNE measurement of $\delta_{\rm CP}$ as a function of its true value 20
1.9 Resolution of DUNE measurements of $\delta_{\rm CP}$ and $\sin^2 2\theta_{13}$, as a function of exposure . . . 21
1.10 Resolution of DUNE measurements of $\sin^2 2\theta_{23}$ and Δm^2_{32}, as a function of exposure . . 21
1.11 Two-dimensional 90% C.L. regions in $\sin^2 2\theta_{13}/\sin^2\theta_{23}$ vs. $\delta_{\rm CP}$ 22
1.12 Sensitivity of determination of the θ_{23} octant as a function of $\sin^2\theta_{23}$ 23
1.13 Reconstructed dE/dx of protons and muons in ProtoDUNE-SP 24
1.14 Fit to three supernova neutrino pinched-thermal spectrum parameters 26
1.15 Supernova direction determination from $\nu - e$ elastic scattering events 27
1.16 Sensitivity to effective mixing angle $\theta_{\mu e}$ from a DUNE sterile neutrino analysis 28
1.17 Projected sensitivity to BSM contributions to neutrino trident events 29

List of Tables

1.1 ν_e and $\bar{\nu}_e$ appearance yields 14
1.2 ν_μ and $\bar{\nu}_\mu$ disappearance yields 15
1.3 Projected DUNE oscillation physics milestones 16

Chapter 1

DUNE Physics

This chapter provides a brief introduction to DUNE physics. The text below closely follows the presentation in the introductory chapters of Volume II, where many more details may be found.

Presented here in summary form are (1) the scientific goals and opportunities, (2) the methodologies we have employed to evaluate the capabilities of DUNE to realize the science, and (3) the corresponding results for selected program elements.

1.1 Goals of the DUNE Science Program

The primary goals and ancillary science program elements listed in the previous chapter represent discovery opportunities at the forefront of particle physics and astrophysics. The Deep Underground Neutrino Experiment (DUNE) has been designed to capitalize on these opportunities with a unique set of experimental conditions and capabilities. In this section we elaborate on elements of the science program that motivate the operating principles of DUNE that were presented in the previous chapter.

The focus of the presentation here is on physics opportunities offered by the DUNE far detector (FD). The DUNE near detector (ND) will have its own physics program, only a small portion of which is covered here. The full ND physics program will be described in the ND conceptual design report (CDR), which is in progress as of this writing.

1.1.1 Neutrino Oscillations: Masses, Mixing Angles and CP Violation

Neutrino oscillations imply nonzero neutrino masses and flavor-mixing in the leptonic charged current (CC) interactions. The nonzero neutrino mass is among the most important discoveries in fundamental particle physics of the twenty-first century. Understanding the mechanism behind

nonzero neutrino masses is among the unresolved mysteries that drive particle physics today; they remain one of the few unambiguous facts that point to the existence of new particles and interactions, beyond those that make up the remarkable standard model of particle physics.

Almost all neutrino data can be understood within the three-flavor paradigm with massive neutrinos, the simplest extension of the standard model capable of reconciling theory with observations. It consists of introducing distinct, nonzero, masses for at least two neutrinos, while maintaining the remainder of the standard model. Hence, neutrinos interact only via the standard model CC and neutral current (NC) weak interactions. The neutrino mass eigenstates – defined as ν_1, ν_2, ν_3 with masses, m_1, m_2, m_3, respectively – are distinct from the neutrino CC interaction eigenstates, also referred to as the flavor eigenstates – ν_e, ν_μ, ν_τ, labeled according to the respective charged-lepton e, μ, τ to which they couple in the CC weak interaction. The flavor eigenstates can be expressed as linear combinations of the mass eigenstates: the coefficients of the respective linear combinations define a unitary 3×3 mixing matrix, the Pontecorvo-Maki-Nakagawa-Sakata (PMNS) matrix, as follows:

$$\begin{pmatrix} \nu_e \\ \nu_\mu \\ \nu_\tau \end{pmatrix} = \begin{pmatrix} U_{e1} & U_{e2} & U_{e3} \\ U_{\mu 1} & U_{\mu 2} & U_{\mu 3} \\ U_{\tau 1} & U_{\tau 2} & U_{\tau 3} \end{pmatrix} \begin{pmatrix} \nu_1 \\ \nu_2 \\ \nu_3 \end{pmatrix}. \tag{1.1}$$

Nonzero values for at least some of the off-diagonal elements, coupled with nonzero differences in the masses of ν_1, ν_2 and ν_3, lead to the phenomenon of neutrino oscillations, in which a neutrino – produced in a flavor eigenstate – acquires an oscillating probability of interacting as a different flavor (with an oscillation frequency proportional to the differences of the squares of the neutrino masses, $\Delta m^2_{ij} \equiv m^2_i - m^2_j$).

The PMNS matrix is the leptonic-equivalent of the Cabibbo-Kobayashi-Maskawa matrix (CKM matrix) that describes the CC interactions of quark mass eigenstates. If the neutrinos are Dirac fermions, the PMNS matrix, like the CKM matrix, can be unambiguously parameterized with three mixing angles and one complex phase.[1] By convention [1], the mixing angles are denoted θ_{12}, θ_{13}, and θ_{23}, defined as

$$\sin^2\theta_{12} \equiv \frac{|U_{e2}|^2}{1-|U_{e3}|^2}, \tag{1.2}$$

$$\sin^2\theta_{23} \equiv \frac{|U_{\mu 3}|^2}{1-|U_{e3}|^2}, \tag{1.3}$$

$$\sin^2\theta_{13} \equiv |U_{e3}|^2, \tag{1.4}$$

and one phase $\delta_{\rm CP}$, which in the conventions of [1], is given by

$$\delta_{\rm CP} \equiv -\arg(U_{e3}). \tag{1.5}$$

For values of $\delta_{\rm CP} \neq 0, \pi$, and assuming none of the $U_{\alpha i}$ vanish ($\alpha = e, \mu, \tau$, $i = 1, 2, 3$), the neutrino mixing matrix is complex and charge parity (CP)-invariance is violated in the lepton sector. This, in turn, manifests itself as different oscillation probabilities, in vacuum, for neutrinos and antineutrinos: $P(\nu_\alpha \to \nu_\beta) \neq P(\bar{\nu}_\alpha \to \bar{\nu}_\beta)$, $\alpha, \beta = e, \mu, \tau$, $\alpha \neq \beta$.

[1] Additional nontrivial phases are present if neutrinos are Majorana fermions, but these do not affect oscillations at an observable level.

The central aim of the worldwide program of neutrino experiments past, present and planned, is to explore the phenomenology of neutrino oscillations in the context of the three-flavor paradigm, and, critically, to challenge its validity with measurements at progressively finer levels of precision. The world's neutrino data significantly constrain all of the oscillation parameters in the three-flavor paradigm, but with precision that varies considerably from one parameter to the next.

Critical questions remain open. The neutrino mass ordering – whether ν_3 is the heaviest ("normal" ordering) or the lightest ("inverted" ordering) – is unknown. Current data prefer the normal ordering, but the inverted one still provides a decent fit to the data. The angle θ_{23} is known to be close to the maximal-mixing value of $\pi/4$, but assuming it is not exactly so, the octant (whether $\sin^2\theta_{23} < 0.5$ [$\theta_{23} < \pi/4$] or $\sin^2\theta_{23} > 0.5$ [$\theta_{23} > \pi/4$]) is also unknown. The value of $\delta_{\rm CP}$ is only poorly constrained. While positive values of $\sin\delta_{\rm CP}$ are disfavored, all $\delta_{\rm CP}$ values between π and 2π, including the CP-conserving values $\delta_{\rm CP} = 0, \pi$, are consistent with the world's neutrino data.[2] That the best fit to the world's data favors large charge-parity symmetry violation (CPV) is intriguing, providing further impetus for experimental input to resolve this particular question. It is central to the DUNE mission that all of the questions posed here can be addressed by neutrino oscillation experiments.

Conventional horn-focused beams, where either ν_μ or $\bar{\nu}_\mu$ is the dominant species (depending on horn current polarity), provide access to these questions for experiments at long baselines as in the case of DUNE and the Long-Baseline Neutrino Facility (LBNF). By virtue of the near-maximal value of θ_{23}, oscillations are mainly in the mode $\nu_\mu \to \nu_\tau$. For realizable baselines, this channel is best studied by measuring the ν_μ disappearance probability as a function of neutrino energy rather than through direct observation of ν_τ appearance. This is because oscillation maxima occur at energies below the threshold for τ-lepton production in ν_τ CC interactions in the detector. On the other hand, the sub-dominant $\nu_\mu \to \nu_e$ channel is amenable to detailed study through the energy dependence of the ν_e and $\bar{\nu}_e$ appearance probabilities, which is directly sensitive (in a rather complex way) to multiple PMNS matrix parameters, as described below.

Specifically, the oscillation probability of $\nu_\mu \to \nu_e$ through matter in a constant density approximation is, to first order [3]:

$$\begin{aligned} P(\nu_\mu \to \nu_e) \;\simeq\; & \sin^2\theta_{23}\sin^2 2\theta_{13}\frac{\sin^2(\Delta_{31}-aL)}{(\Delta_{31}-aL)^2}\Delta_{31}^2 \\ & + \sin 2\theta_{23}\sin 2\theta_{13}\sin 2\theta_{12}\frac{\sin(\Delta_{31}-aL)}{(\Delta_{31}-aL)}\Delta_{31}\frac{\sin(aL)}{(aL)}\Delta_{21}\cos(\Delta_{31}+\delta_{\rm CP}) \\ & + \cos^2\theta_{23}\sin^2 2\theta_{12}\frac{\sin^2(aL)}{(aL)^2}\Delta_{21}^2, \end{aligned} \tag{1.6}$$

where $\Delta_{ij} = \Delta m^2_{ij} L/4E_\nu$, $a = G_F N_e/\sqrt{2}$, G_F is the Fermi constant, N_e is the number density of electrons in the Earth, L is the baseline in km, and E_ν is the neutrino energy in GeV. In the equation above, both $\delta_{\rm CP}$ and a switch signs in going from the $\nu_\mu \to \nu_e$ to the $\bar{\nu}_\mu \to \bar{\nu}_e$ channel; i.e., a neutrino-antineutrino asymmetry is introduced both by CPV ($\delta_{\rm CP}$) and the matter effect (a). As is evident from Equation 1.6, the matter effect introduces a sensitivity to the sign of Δ_{31}, which specifies the neutrino mass ordering. The origin of the matter effect asymmetry is

[2] It should be noted that recent results from the T2K experiment [2] show only marginal consistency with CP-conserving values of $\delta_{\rm CP}$.

simply the presence of electrons and absence of positrons in the Earth. In the few-GeV energy range, the asymmetry from the matter effect increases with baseline as the neutrinos pass through more matter; therefore an experiment with a longer baseline will be more sensitive to the neutrino mass ordering. For baselines longer than ∼1200 km, the degeneracy between the asymmetries from matter and CPV effects can be resolved [4].

The electron neutrino appearance probability, $P(\nu_\mu \rightarrow \nu_e)$, is plotted in Figure 1.1 at a baseline of 1300 km as a function of neutrino energy for several values of $\delta_{\rm CP}$. As this figure illustrates, the value of $\delta_{\rm CP}$ affects both the amplitude and phase of the oscillation. The difference in probability amplitude for different values of $\delta_{\rm CP}$ is larger at higher oscillation nodes, which correspond to energies less than 1.5 GeV. Therefore, a broadband experiment, capable of measuring not only the rate of ν_e appearance but of mapping out the spectrum of observed oscillations down to energies of at least 500 MeV, is desirable.

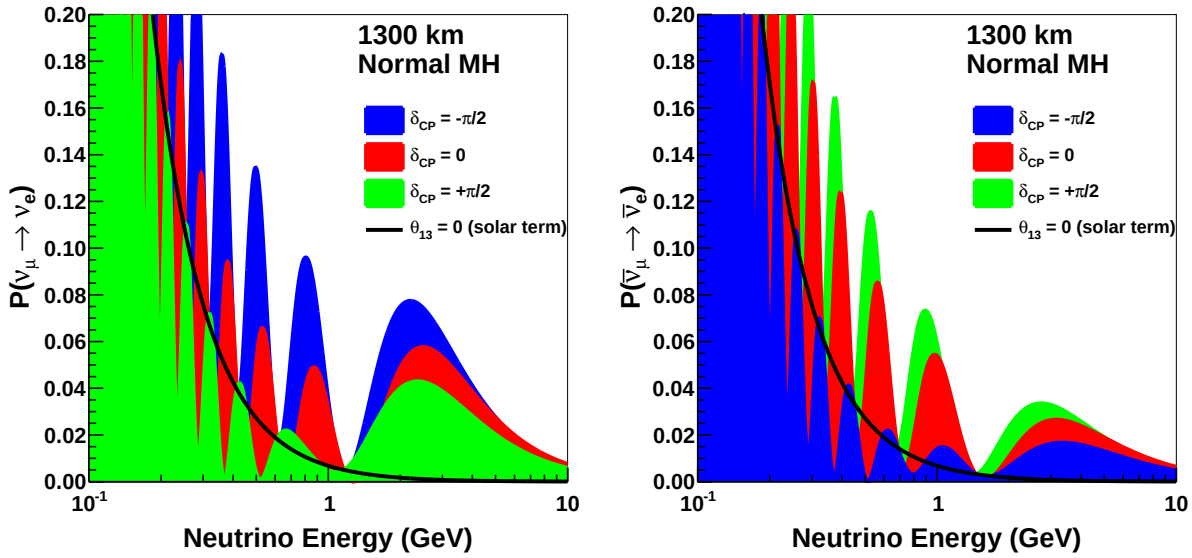


Figure 1.1: The appearance probability at a baseline of 1300 km, as a function of neutrino energy, for $\delta_{\rm CP} = -\pi/2$ (blue), 0 (red), and $\pi/2$ (green), for neutrinos (left) and antineutrinos (right), for normal ordering. The black line indicates the oscillation probability if θ_{13} were equal to zero. Note that the DUNE FD will be built at a baseline of 1300 km.

DUNE is designed to address the questions articulated above, to over-constrain the three-flavor paradigm, and to reveal what may potentially lie beyond. Even if consistency is found, the precision measurements obtained by DUNE will have profound implications. As just one example, the discovery of CPV in neutrino oscillations would provide strong circumstantial evidence for the leptogenesis mechanism as the origin of the baryon asymmetry of the universe.

Going further, the patterns defined by the fermion masses and mixing parameters have been the subject of intense theoretical activity for the last several decades. Grand unified theories (GUTs) posit that quarks and leptons are different manifestations of the same fundamental entities, and thus their masses and mixing parameters are related. Different models make different predictions but, in order to compare different possibilities, it is important that lepton mixing parameters be known as precisely as quark mixing parameters. To enable equal-footing comparisons between

quark and lepton mixing it is required that the mixing angles be determined at the few percent level while $\delta_{\rm CP}$ should be measured at the 10% level or better. Measurements with precision at these levels are expected from DUNE for the mixing angles θ_{23} and θ_{13}, and the CP phase $\delta_{\rm CP}$. These measurements will thus open a new era of flavor physics, with the potential to offer insight on deep questions on which the standard model (SM) is essentially silent.

1.1.2 Baryon Number Violation

Are protons stable? Few questions within elementary particle physics can be posed as simply and at the same time have implications as immediate. The apparent stability of protons suggests that baryon number is conserved in nature, although no known symmetry requires it to be so. Indeed, baryon number conservation is implicit in the formulation of the SM Lagrangian, and thus observation of baryon-number violating (BNV) processes such as nucleon decay or neutron-antineutron oscillation would be evidence for physics beyond the SM. On the other hand, continued non-observation of BNV processes will demand an answer to what new symmetry is at play that forbids them.

Especially compelling is that the observation of BNV processes could be the harbinger for grand unified theories, in which strong, weak and electromagnetic forces are unified. Numerous GUT models have been proposed, each with distinct features. Yet, BNV processes are expected on general grounds, and it is a feature of many models that nucleon decay channels can proceed at experimentally accessible rates. This is illustrated for several key nucleon decay channels relevant for DUNE in Figure 1.2, along with existing experimental limits.

Given the scale of energy deposition in the few hundred MeV to few GeV range, a detector optimized for neutrino oscillation physics at long baselines is naturally well suited for sensitive searches for nucleon decay and neutron-antineutron oscillations. Thanks to the excellent imaging, calorimetric and particle identification capabilities of the liquid argon time-projection chamber (LArTPC), backgrounds can in principle be reduced below the single-event level for key nucleon decay channels at exposures where other detector technologies are no longer background-free. On the other hand, a challenge presented by an argon-based detector is the impact of final-state interactions (FSI) on nucleon decay event reconstruction, which is expected to be more severe than for detectors based on water or liquid scintillator, for example. On balance, however, should nucleon decays occur at rates not far beyond current best limits, a handful of candidate events could be observed by DUNE in a given decay mode. For the case of zero observed candidates, DUNE has the potential to set partial lifetime limits for favorable channels at the 10^{34} year level, as indicated in Section 1.3.2.

1.1.3 Supernova Neutrino Bursts

The burst of neutrinos [6, 7] from the celebrated core-collapse supernova 1987A in the Large Magellanic Cloud, about 50 kiloparsecs (kpc) from Earth, heralded the era of extragalactic neutrino astronomy. The few dozen recorded $\bar{\nu}_e$ events have confirmed the basic physical picture of core collapse and yielded constraints on a wide range of new physics [8, 9].

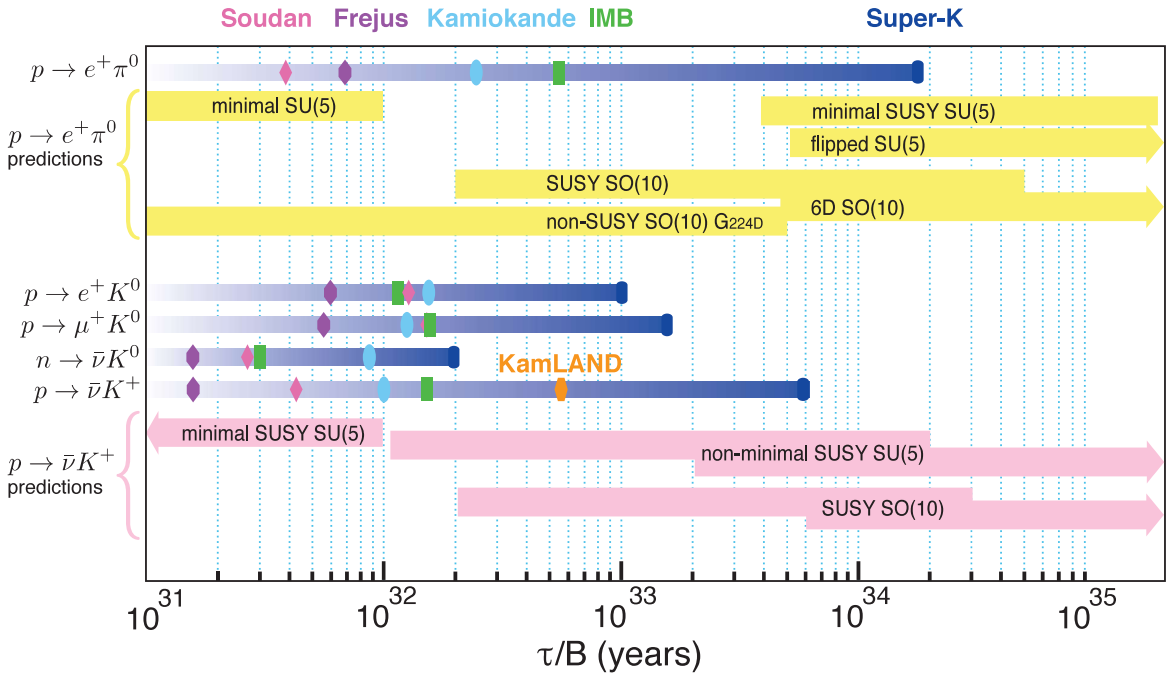


Figure 1.2: Summary of nucleon decay experimental lifetime limits from past or currently running experiments for several modes, and the model predictions for the lifetimes in the two modes $p \to e^+\pi^0$ and $p \to K^+\overline{\nu}$. The limits shown are 90% confidence level (CL) lower limits on the partial lifetimes, τ/B, where τ is the total mean life and B is the branching fraction. Updated from [5].

Core-collapse supernovae within a few hundred kpc of Earth – within our own galaxy and nearby – are quite rare on a human timescale. They are expected once every few decades in the Milky Way (within about 20 kpc), and with a similar rate in Andromeda, about 700 kpc away. These core collapses should be common enough to have a reasonable chance of occurring during the few-decade long lifetime of a typical large-scale neutrino detector.

It is important that at least one module of the DUNE FD be online at all times to observe this unpredictable and spectacular event, if and when it occurs. The rarity of these events makes it all the more critical for the community to be prepared to capture every last bit of information from them.

The information in a supernova neutrino burst (SNB) available in principle to be gathered by experimentalists is the *flavor, energy and time structure* of a several-tens-of-second-long, all-flavor, few-tens-of-MeV neutrino burst [10, 11]. Imprinted on the neutrino spectrum as a function of time is information about the progenitor, the collapse, the explosion, and the remnant, as well as information about neutrino parameters and potentially exotic new physics. Neutrino energies and flavor content of the burst can be measured only imperfectly, due to the intrinsic nature of the weak interactions of neutrinos with matter, as well as due to imperfect detection resolution in any real detector. For example, SNB energies are below CC threshold for ν_μ, ν_τ, $\bar{\nu}_\mu$, and $\bar{\nu}_\tau$ (collectively ν_x), which represent two-thirds of the flux; so these flavors are accessible only via NC interactions, which tend to have low cross sections and indistinct detector signatures. These issues make a comprehensive unfolding of neutrino flavor, time and energy structure from the observed

interactions a challenging problem.

The core-collapse neutrino signal starts with a short, sharp *neutronization* (or *break-out*) burst primarily composed of ν_e. These neutrinos are messengers of the shock front breaking through the neutrinosphere (the surface of neutrino trapping): when this happens, iron is disintegrated, the neutrino scattering cross section drops, and the lepton number trapped just below the original neutrinosphere is suddenly released. This quick and intense burst is followed by an *accretion phase* lasting some hundreds of milliseconds, depending on the progenitor star mass, as matter falls onto the collapsed core and the shock is stalled at the distance of perhaps $\sim$ 200 km. The gravitational binding energy of the accreting material is powering the neutrino luminosity during this stage. The later *cooling phase* over $\sim$10 seconds represents the main part of the signal, over which the proto-neutron star sheds its trapped energy.

The flavor content and spectra of the neutrinos emitted from the neutrinosphere change throughout these phases, and the supernova's evolution can be followed with the neutrino signal. Some fairly generic features of these emitted neutrino fluxes are illustrated in Figure 1.3.

In the world's current supernova neutrino flavor sensitivity portfolio [13, 10], the sensitivity is primarily to electron antineutrino flavor, via inverse beta decay. There is only minor sensitivity to the ν_e component of the flux, which carries with it particularly interesting information content of the burst (e.g., neutronization burst neutrinos are created primarily as ν_e). While there is some ν_e sensitivity in existing and other planned detectors via elastic scattering on electrons and via subdominant channels on nuclei, statistics are relatively small, and it can be difficult to disentangle the flavor content. It is in this respect that an experiment with an argon target such as DUNE will be especially valuable, since the dominant process in this case is ν_e CC scattering.

1.1.4 Additional Beyond-Standard-Model Physics Signatures

The capabilities that enable access to the physics program described in the previous sections open a myriad of opportunities to search for evidence of physics beyond the standard model. Below we list the identified opportunities that we have investigated. Projected sensitivities are shown later in this chapter for only a few of these opportunities; we refer the reader to Volume II, DUNE Physics, for a more complete demonstration of the potential impact of DUNE's searches for BSM phenomena, which can justifiably be considered as prominent ancillary elements of the DUNE science program. At the same time, it is important to note that new physics may appear in ways that have not yet been considered: history has repeatedly shown that nature can reward new experimental approaches and sensitive detectors with the appearance of entirely unanticipated phenomena.

Opportunities in BSM physics that have been considered as elements of the DUNE science program include:

Search for active-sterile neutrino mixing: DUNE is sensitive over a broad range of potential sterile neutrino mass splittings by looking for disappearance of CC and NC interactions over the long distance separating the ND and FD, as well as over the short baseline of the ND. With a longer

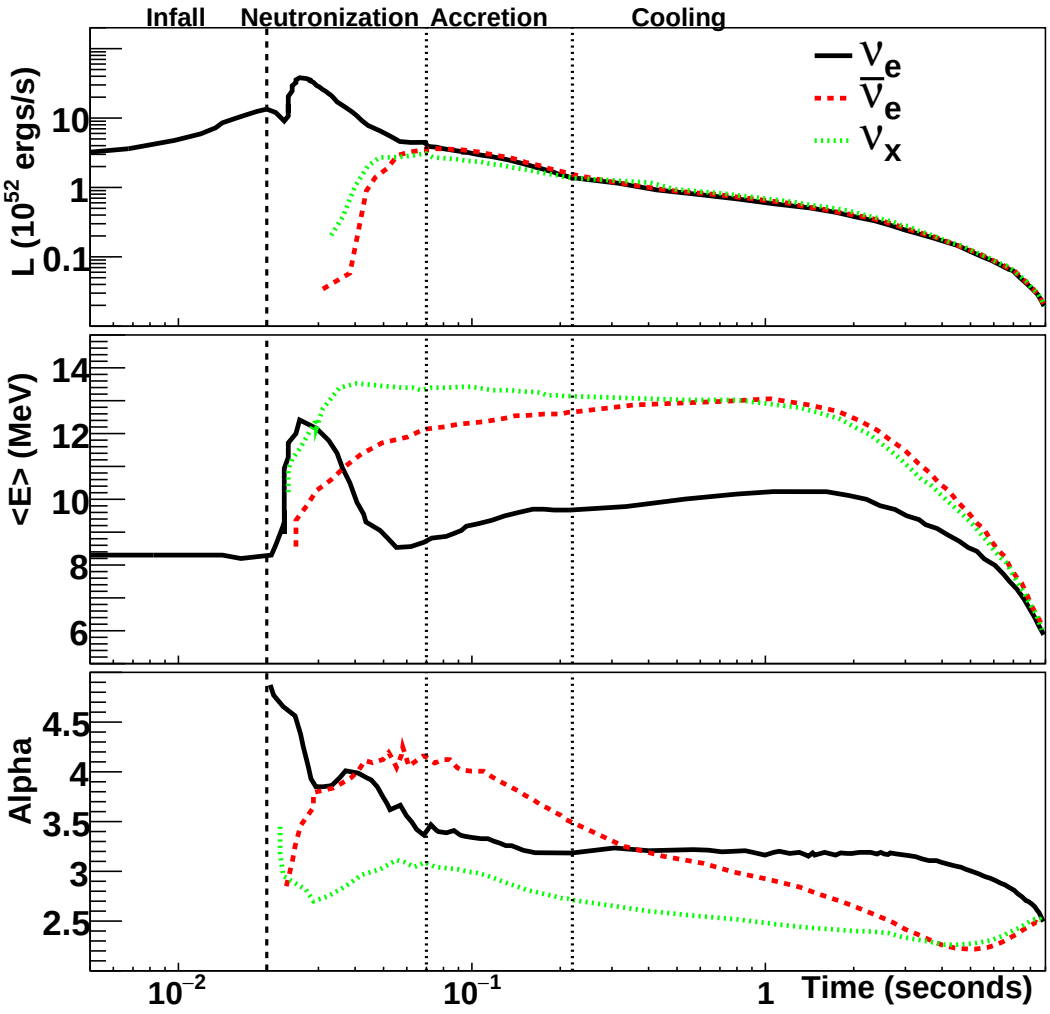


Figure 1.3: Expected time-dependent signal for a specific flux model for an electron-capture supernova [12] at 10 kpc. No oscillations are assumed; the effect of neutrino flavor transitions under different mass ordering assumptions can be dramatic and is described in Volume II Chapter 7. Note that ν_x refers to ν_μ, ν_τ, $\bar{\nu}_\mu$, and $\bar{\nu}_\tau$ collectively. The top plot shows the luminosity as a function of time (ν_x is the sum of all, the second plot shows average neutrino energy, and the third plot shows the α (pinching) parameter. The vertical dashed line at 0.02 seconds indicates the time of core bounce, and the vertical lines indicate different eras in the supernova evolution. The leftmost time interval indicates the infall period. The next interval, from core bounce to 50 ms, is the neutronization burst era, in which the flux is composed primarily of ν_e. The next period, from 50 to 200 ms, is the accretion period. The final era, from 0.2 to 9 seconds, is the proto-neutron-star cooling period. The general features are qualitatively similar for most core-collapse supernovae.

baseline, a more intense beam, and a high-resolution large-mass FD, compared to previous experiments, DUNE provides a unique opportunity to improve significantly on the sensitivities of the existing probes, and greatly enhance the ability to map the extended parameter space if a sterile neutrino is discovered.

Searches for non-unitarity of the PMNS matrix: Deviation from unitarity of the 3×3 PMNS matrix due to extra heavy neutrino states may be observable. Parameters characterizing the degree of non-unitarity can become sizable as the masses of the new states decrease.

Searches for nonstandard interactions (NSIs): NSIs affecting neutrino propagation through the Earth can significantly modify the data to be collected by DUNE as long as the new physics parameters are large enough. If the DUNE data are consistent with standard oscillations for three massive neutrinos, interaction effects of order 0.1 G_F can be ruled out at DUNE.

Searches for violation of Lorentz symmetry or charge, parity, and time reversal symmetry (CPT): DUNE can improve the present limits on Lorentz and CPT violation in the neutrino sector by several orders of magnitude, contributing an important experimental test of these fundamental assumptions underlying quantum field theory.

Studies of neutrino trident production: Interactions of neutrinos with the Coulomb field of a nucleus can lead to final states with a lepton-pair accompanying the lepton from the neutrino interaction vertex. With a predicted annual rate of over 100 dimuon neutrino trident interactions at the ND, DUNE will be able to measure deviations from the SM rates and test the presence of new gauge symmetries.

Search for light-mass dark matter (LDM): The lack of evidence for weakly-interacting massive particle (WIMP) dark matter (DM) candidates from direct detection and LHC experiments has resulted in a reconsideration of the WIMP paradigm, and has revitalized the effort to search for LDM candidates of around a GeV or below in mass. High-flux neutrino beam experiments, such as DUNE, have been shown to provide coverage of DM+mediator parameter space that cannot be covered by either direct detection or collider experiments. DM particles can be detected in the ND through NC-like interactions either with electrons or nucleons in the detector material and enable DUNE's search for LDM to be competitive and complementary to other experiments.

Search for boosted dark matter (BDM): Using its large FD, DUNE will be able to search for BDM. In these models there are several DM particles with different masses and properties concerning their interactions with SM particles. DUNE will search for such particles as generally produced anywhere in the cosmos or specifically through annihilation in the core of the sun, allowing competitive results for both production scenarios

Search for heavy neutral leptons (HNLs): HNLs in the context of the νMSM model with masses less than 2 GeV can be produced in the beam-dump of the proton beam to generate the DUNE neutrino beam. The ND data can be used to search for HNL decays, and competitive results with other present and proposed facilities can be obtained.

1.2 Summary of Assumptions and Methods Employed

Scientific capabilities are determined assuming that DUNE is configured according to the general parameters described in Section **??**. Further assumptions regarding the neutrino beam and detector systems, and their deployment are stated here in Sections 1.2.1 and 1.2.2.

Determination of experimental sensitivities relies on the modeling of the underlying physics and background processes, as well as the detector response, including calibration and event reconstruction performance and the utilization of data analysis techniques and tools. Section 1.2.3 gives a brief discussion of the strategies employed.

1.2.1 Beam and Detector

Physics sensitivities are based on the optimized design of a 1.2 MW neutrino beam and corresponding protons-on-target per year assumed to be 1.1×10^{21} POT. These numbers assume a combined uptime and efficiency of the Fermi National Accelerator Laboratory (Fermilab) accelerator complex and the LBNF beamline of 56%.[3]

For the neutrino oscillation physics program, it is assumed that equal exposures (time-integrated beam power times fiducial mass) are obtained with both horn current polarities, and therefore with the corresponding mix of primarily ν_μ and $\bar{\nu}_\mu$ data samples.

It is assumed that the DUNE FD will include some combination of the different 10 kt fiducial volume implementations – single-phase (SP) or dual-phase (DP) – of the LArTPC concept for which technical designs have been developed. For much of the science program it is expected that the capabilities of the two proposed FD module implementations will be comparable. As a result of the current state of reconstruction and analysis software development (see Section 1.2.3), the physics sensitivity studies reported in this technical design report (TDR) are based on the SP LArTPC implementation, documented in full in Volume IV.

It is also assumed that validation of the DUNE FD designs will come from data and operational experience acquired with the large-scale ProtoDUNE detectors staged at the European Organization for Nuclear Research (CERN), including single-particle studies of data obtained in test-beam running.

The ND for DUNE has been under active development, and a CDR is in preparation. Correspondingly, the descriptions in this TDR are consistent with this level of development.

[3] This projection, from which one year of LBNF beam operations (live time) can be expressed as 1.7×10^7 seconds, is based on extensive experience with intense neutrino beams at Fermilab, and in particular the NuMI beam line, which incorporates elements like those in the proposed LBNF beamline design and faces similar operating conditions.

1.2.2 Deployment Scenario

Where presented as a function of calendar year, sensitivities are calculated with the following assumed deployment plan, which is based on a technically limited schedule:

- Start of beam run: Two FD module volumes for total fiducial mass of 20 kt, 1.2 MW beam;
- After one year: Add one FD module volume for total fiducial mass of 30 kt;
- After three years: Add one FD module volume for total fiducial mass of 40 kt; and
- After six years: Upgrade to 2.4 MW beam.

1.2.3 Simulation, Reconstruction, and Data Analysis Tools

The development of algorithms and software infrastructure needed to carry out physics sensitivity studies has been an active effort within DUNE and the associated scientific community. Significant progress has been made: event reconstruction codes can be run on fully simulated neutrino interaction events in DUNE FD modules; the DUNE computing infrastructure allows high-statistics production runs; and end-user interfaces are functioning. Robust end-to-end analyses not previously possible have now been performed and are being reported in this document.

For some aspects – for example, beamline modeling and GeV-scale neutrino interaction simulations – well-developed and validated (with data) software packages have been available throughout much of DUNE's design phase. For others, corresponding tools did not exist and needed to be either developed from scratch or adapted with substantial modifications from other experimental programs. Concurrent with these development efforts, interim descriptions such as parametric detector response modeling, necessarily simple but based on reasonable extrapolation from experience and dedicated studies, were employed to assess physics capabilities. Even for the case of the better-developed tools – again, neutrino interaction modeling is a good example – significant incremental improvements have been made as data from neutrino experiments and other sources have become available and as theoretical understandings have advanced.

As a result of the rapid pace of development as well as practical considerations including human resource availability, different levels of rigor have been applied in the evaluation of physics capabilities for different elements of the program. The strategy adopted for this TDR has been to hold the primary elements of the program to the highest standard of rigor, involving direct analysis of fully simulated data, using actual event reconstruction codes and analysis tools that could be applied to real data from DUNE FD modules. For other elements of the program, sensitivities use realistic beam and physics simulations, but employ parametric detector response models in place of full reconstruction.

The implementation of this strategy comes with caveats and clarifications that are discussed in the corresponding chapters of Volume II. We mention some of these here.

- In the case of the long-baseline oscillation physics program, this approach requires a com-

bination of the full end-to-end analysis of simulated FD data with the concurrent analysis of simulated data from ND systems to capture in a realistic way the level of control over systematic errors. Given the current state of development of the DUNE ND design and corresponding analysis tools, it has been necessary to employ parametric detector response modeling for ND components.

- In the case of the nucleon decay searches, reconstruction and analysis tools dedicated to addressing the particular challenges presented are not as well developed as in the case of the beam-based oscillation physics program. Effort is ongoing to improve the performance of these tools.
- The SNB program relies on reconstruction of event signatures from LArTPC signals generated by low-energy (MeV-scale) particles (electrons and de-excitation gammas). Full simulation and reconstruction is used for some studies, such as for those demonstrating the supernova pointing capability of DUNE. For other studies, a modified strategy is employed in order to efficiently explore model space: reconstruction metrics (resolution smearing matrices, for example) are derived from analysis of fully simulated and reconstructed low-energy particles and events in the FD, and are applied to understanding the mean detector response over a range of signal predictions.
- For scientific program elements where analysis of fully reconstructed simulated data has not yet been performed, the parametric response models used for the analyses presented here have been well characterized with dedicated studies and incorporation of results from other experiments. The demonstration of sensitivities for the long-baseline oscillation physics program (with full reconstruction) that are comparable to those previously obtained based on parametric response validates this approach.

1.3 Selected Results from Sensitivity Studies

In this section, selected sensitivity projections from the central elements of the DUNE science program are presented. This selection is intended to convey just the headlines from what is an extensive and diverse program of frontier science.

1.3.1 CPV in the Neutrino Sector and Precise Oscillation Parameter Measurements

The key strength of the DUNE design concept is its ability to robustly measure the oscillation patterns of ν_μ and $\bar{\nu}_\mu$ over a range of energies spanning the first and second oscillation maxima.

This is accomplished by a coordinated analysis of the reconstructed ν_μ, $\bar{\nu}_\mu$, ν_e, and $\bar{\nu}_e$ energy spectra in near and far detectors, incorporating data collected with forward (neutrino-dominated) and reverse (antineutrino-dominated) horn current polarities.

The statistical power of DUNE relative to the current generation of long-baseline oscillation exper-

iments is a result of many factors including (1) on-axis operations, (2) the LBNF beam power, (3) long-baseline and correspondingly high energy oscillation maxima and strong separation of normal and inverted neutrino mass ordering scenarios, (4) detector mass, and (5) event reconstruction and selection capabilities. Tables 1.1 and 1.2 give the expected event yields for the appearance (ν_e and $\bar{\nu}_e$) and disappearance (ν_μ and $\bar{\nu}_\mu$) channels, respectively, after seven years of operation. For these estimates, $\delta_{\rm CP} = 0$ is assumed, and values for other parameters are taken from the NuFIT 4.0 [14, 15] global fit to world neutrino data. (See also [16] and [17] for other recent global fits.) The DUNE ν_e and $\bar{\nu}_e$ event yields represent order-of-magnitude increases relative to those in the current NOvA [18] and T2K [19, 2] data samples, while the corresponding increases are even larger for the ν_μ and $\bar{\nu}_\mu$ channels thanks to DUNE's on-axis exposure to the LBNF beam. Figures 1.4 and 1.5 show the corresponding distributions in reconstructed neutrino energy.

Table 1.1: ν_e and $\bar{\nu}_e$ appearance yields: Integrated yield of selected ν_e CC-like events between 0.5 and 8.0 GeV assuming 3.5-year (staged) exposures in the neutrino-beam and antineutrino-beam modes. The signal yields are shown for both normal mass ordering (NO) and inverted mass ordering (IO), and all the background yields assume normal mass ordering. All the yields assume $\delta_{\rm CP} = 0$, and NuFIT 4.0 [14, 15] values for other parameters.

	Expected Events (3.5 years staged per mode)	
	ν mode	$\bar{\nu}$ mode
ν_e signal NO (IO)	1092 (497)	76 (36)
$\bar{\nu}_e$ signal NO (IO)	18 (31)	224 (470)
Total signal NO (IO)	1110 (528)	300 (506)
Beam $\nu_e + \bar{\nu}_e$ CC background	190	117
NC background	81	38
$\nu_\tau + \bar{\nu}_\tau$ CC background	32	20
$\nu_\mu + \bar{\nu}_\mu$ CC background	14	5
Total background	317	180

Experimental sensitivities were evaluated based on the methodologies described in the preceding section, including incorporation of ND simulations and uncertainties from all known sources of systematic error. Considerable attention and sophistication has been applied to the treatment of systematic errors and the crucial role of the ND, both of which are documented in Volume II, DUNE Physics.

A summary of representative sensitivity milestones for neutrino mass ordering and CPV discovery, as well as precision on $\delta_{\rm CP}$ and $\sin^2 2\theta_{13}$ is given in Table 1.3. The ultimate level of precision that can be obtained on oscillation parameters highlights the point that DUNE will provide crucial input for flavor physics: Patterns required by particular symmetries underlying fermion masses and mixing angles may appear. The unitarity of the neutrino mixing matrix can be tested directly through comparisons of $\sin^2 2\theta_{13}$ with the value obtained from reactor experiments. In conjunction with $\sin^2 2\theta_{13}$ and other parameters, the precise value of $\delta_{\rm CP}$ can constrain models of leptogenesis that are leading candidates for explanation of the baryon asymmetry of the universe.

The milestones presented in Table 1.3 form a coarse snapshot of the DUNE program in oscillation physics, demonstrating the prospects for important results throughout the lifetime of the exper-

Table 1.2: ν_μ and $\bar{\nu}_\mu$ disappearance yields: Integrated yield of selected ν_μ CC-like events between 0.5 and 8.0 GeV assuming a 3.5-year (staged) exposure in the neutrino-beam mode and antineutrino-beam mode. The yields are shown for normal mass ordering and $\delta_{\rm CP} = 0$.

	Expected Events (3.5 years staged)
ν mode	
ν_μ Signal	6200
$\bar{\nu}_\mu$ CC background	389
NC background	200
$\nu_\tau + \bar{\nu}_\tau$ CC background	46
$\nu_e + \bar{\nu}_e$ CC background	8
$\bar{\nu}$ mode	
$\bar{\nu}_\mu$ signal	2303
ν_μ CC background	1129
NC background	101
$\nu_\tau + \bar{\nu}_\tau$ CC background	27
$\nu_e + \bar{\nu}_e$ CC background	2

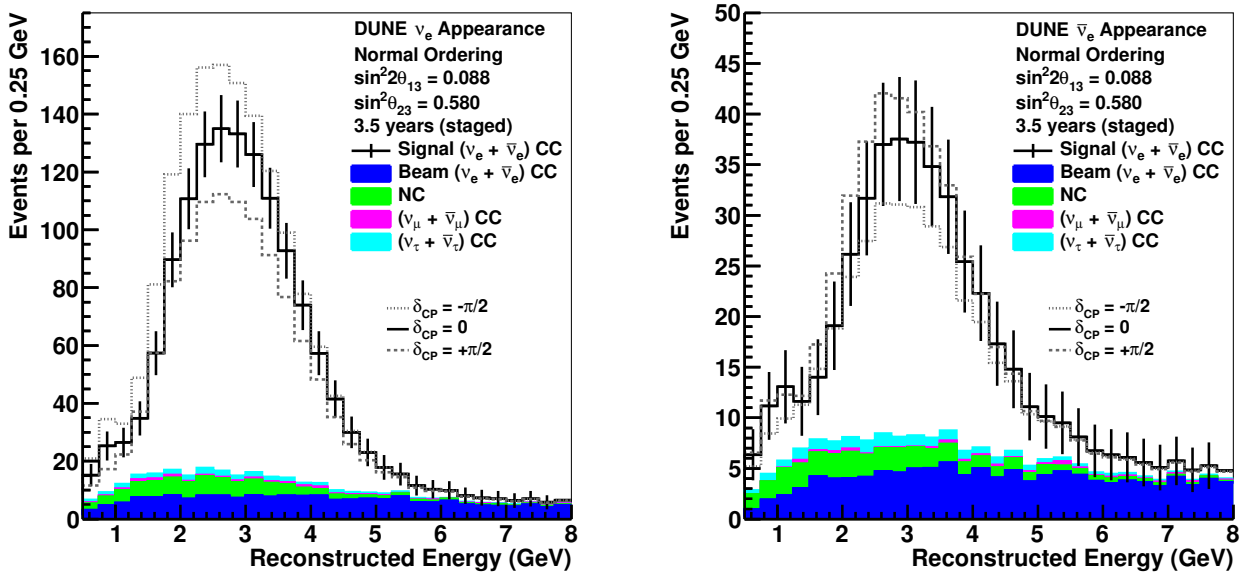


Figure 1.4: ν_e and $\bar{\nu}_e$ appearance spectra: Reconstructed energy distribution of selected ν_e CC-like events assuming 3.5 years (staged) running in the neutrino-beam mode (left) and antineutrino-beam mode (right), for a total of seven years (staged) exposure. The plots assume normal mass ordering and include curves for $\delta_{\rm CP} = -\pi/2, 0$, and $\pi/2$.

Table 1.3: Exposure in years, assuming true normal ordering and equal running in neutrino and antineutrino mode, required to reach selected physics milestones in the nominal analysis, using the NuFIT 4.0 [14, 15] best-fit values for the oscillation parameters. As discussed in Volume II, DUNE Physics, Chapter 5, there are significant variations in sensitivity with the value of $\sin^2\theta_{23}$, so the exact values quoted here (using $\sin^2\theta_{23} = 0.580$) are strongly dependent on that choice. The staging scenario presented in Section 1.2.2 is assumed. Exposures are rounded to the nearest "staged" calendar year. For reference, 30, 100, 200, 336, 624, and 1104 kt · MW · year correspond to 1.2, 3.1, 5.2, 7, 10, and 15 staged years, respectively.

Physics Milestone	Exposure (staged years)
5σ mass ordering ($\delta_{\rm CP} = -\pi/2$)	1
5σ mass ordering (100% of $\delta_{\rm CP}$ values)	2
3σ CPV ($\delta_{\rm CP} = -\pi/2$)	3
3σ CPV (50% of $\delta_{\rm CP}$ values)	5
5σ CPV ($\delta_{\rm CP} = -\pi/2$)	7
5σ CPV (50% of $\delta_{\rm CP}$ values)	10
3σ CPV (75% of $\delta_{\rm CP}$ values)	13
$\delta_{\rm CP}$ resolution of 10 degrees ($\delta_{\rm CP} = 0$)	8
$\delta_{\rm CP}$ resolution of 20 degrees ($\delta_{\rm CP} = -\pi/2$)	12
$\sin^2 2\theta_{13}$ resolution of 0.004	15

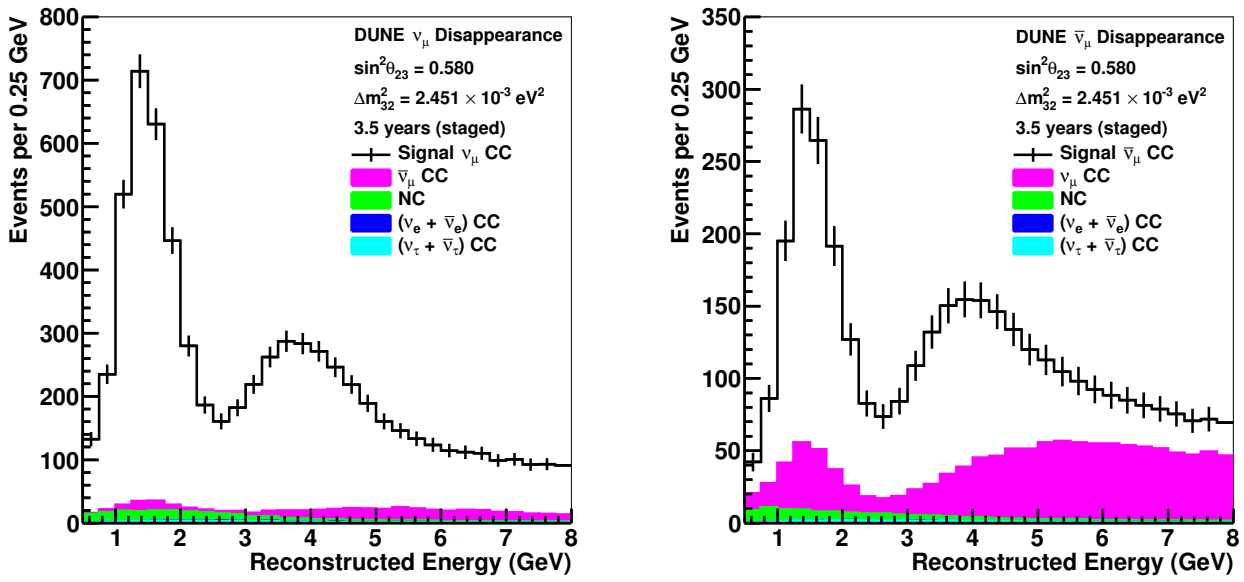


Figure 1.5: ν_μ and $\bar{\nu}_\mu$ disappearance spectra: Reconstructed energy distribution of selected ν_μ CC-like events assuming 3.5 years (staged) running in the neutrino-beam mode (left) and antineutrino-beam mode (right), for a total of seven years (staged) exposure. The plots assume normal mass ordering.

iment. More detail on the sensitivities for the individual program elements is presented in the sections below.

1.3.1.1 Discovery Potential for CPV and Neutrino Mass Ordering

Figure 1.6 illustrates DUNE's ability to distinguish the value of the CP phase $\delta_{\rm CP}$ from CP-conserving values (0 or π) as a function of time in calendar year. These projections incorporate a sophisticated treatment of systematic error, as described in detail in Volume II, DUNE Physics, Chapter 5. Evidence ($> 3\sigma$) for CPV is obtained for favorable values (half of the phase space) of $\delta_{\rm CP}$ after five years of running, leading to a $> 5\sigma$ observation after ten years.

Figure 1.7 shows the significance with which the neutrino mass ordering can be determined for 100% of $\delta_{\rm CP}$ values, and when $\delta_{\rm CP} = -\pi/2$, as a function of exposure in years. The width of the bands show the impact of applying an external constraint on $\sin^2 2\theta_{13}$. As DUNE will be able to establish the neutrino mass ordering at the 5σ level for 100% of $\delta_{\rm CP}$ values after 2-3 years, this plot extends only to seven years.

1.3.1.2 Precision Measurement of Mass and Mixing Parameters

In addition to the discovery potential for neutrino mass ordering and CPV, DUNE will improve the precision on key parameters that govern neutrino oscillations, including: $\delta_{\rm CP}$, $\sin^2 2\theta_{13}$, Δm^2_{31}, $\sin^2\theta_{23}$, and the octant of θ_{23}.

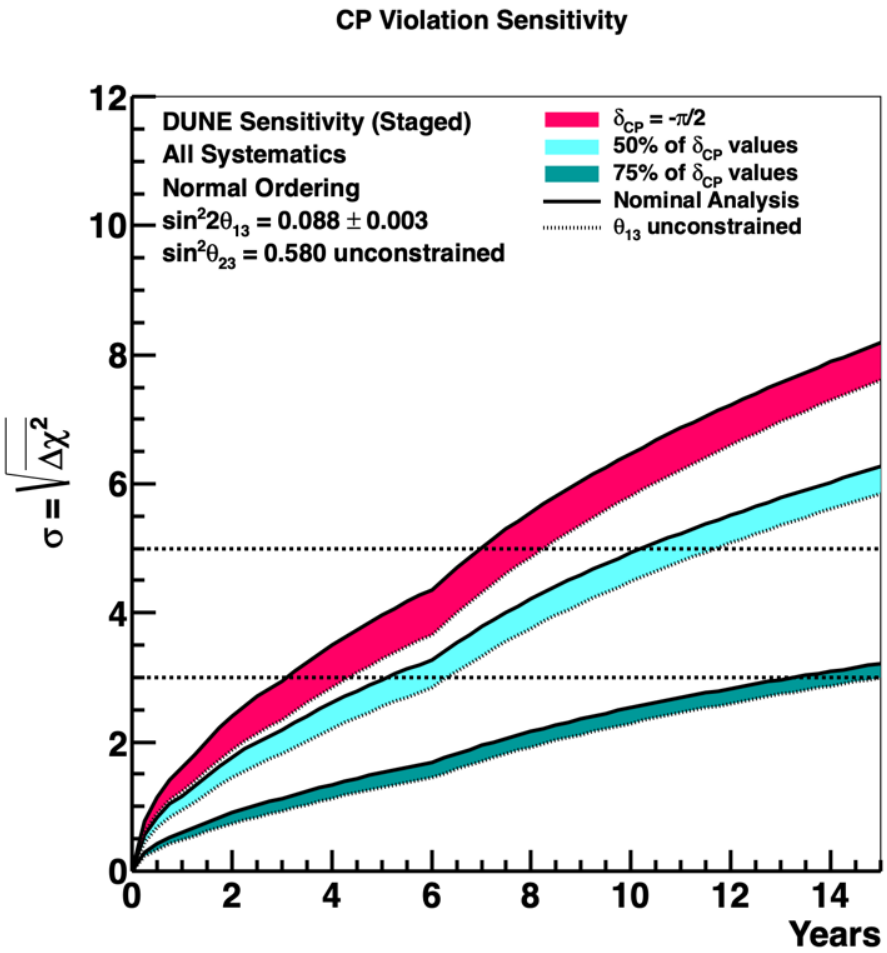


Figure 1.6: Significance of the DUNE determination of CP-violation (i.e.: $\delta_{\rm CP} \neq 0$ or π) for the case when $\delta_{\rm CP} = -\pi/2$, and for 50% and 75% of possible true $\delta_{\rm CP}$ values, as a function of time in calendar years. True normal ordering is assumed. The width of the band shows the impact of applying an external constraint on $\sin^2 2\theta_{13}$.

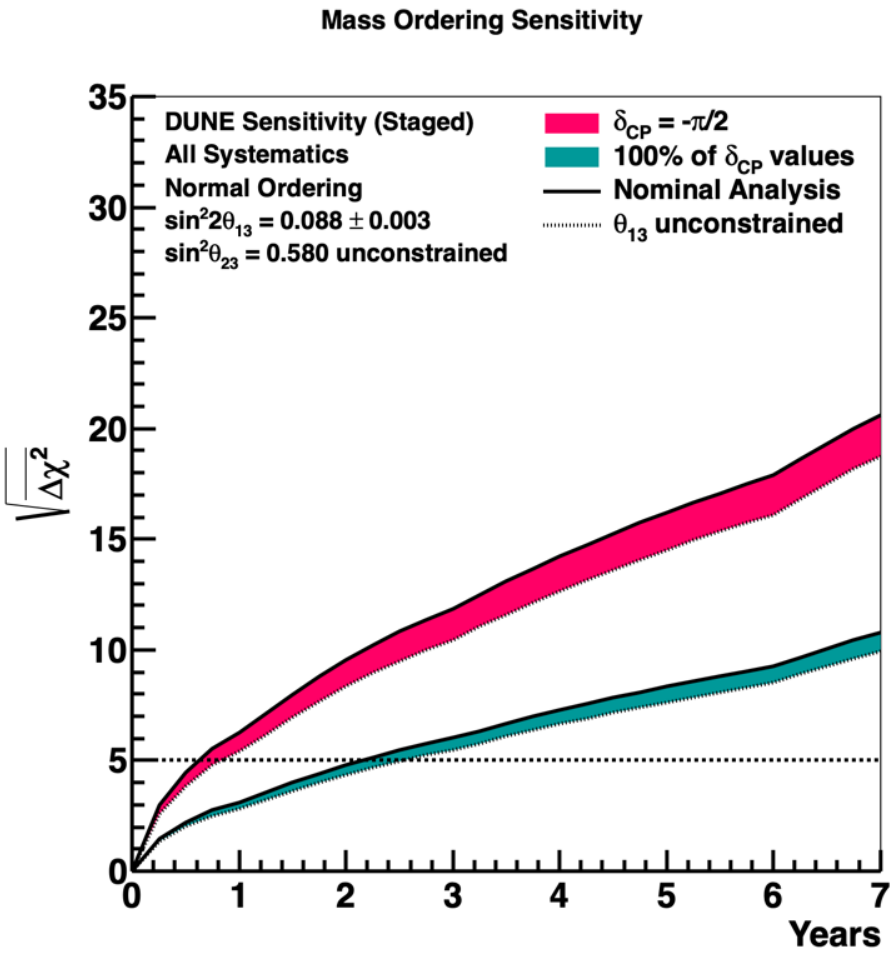


Figure 1.7: Significance of the DUNE determination of the neutrino mass ordering for the case when $\delta_{\rm CP} = -\pi/2$, and for 100% of possible true $\delta_{\rm CP}$ values, as a function of time in calendar years. True normal ordering is assumed. The width of the band shows the impact of applying an external constraint on $\sin^2 2\theta_{13}$.

Figure 1.8 shows the resolution, in degrees, of DUNE's measurement of $\delta_{\rm CP}$ as a function of the true value of $\delta_{\rm CP}$. The resolution of this measurement is significantly better near CP-conserving values of $\delta_{\rm CP}$, compared to maximally CP-violating values. For fifteen years of exposure, resolutions between five and fifteen degrees are possible, depending on the true value of $\delta_{\rm CP}$.

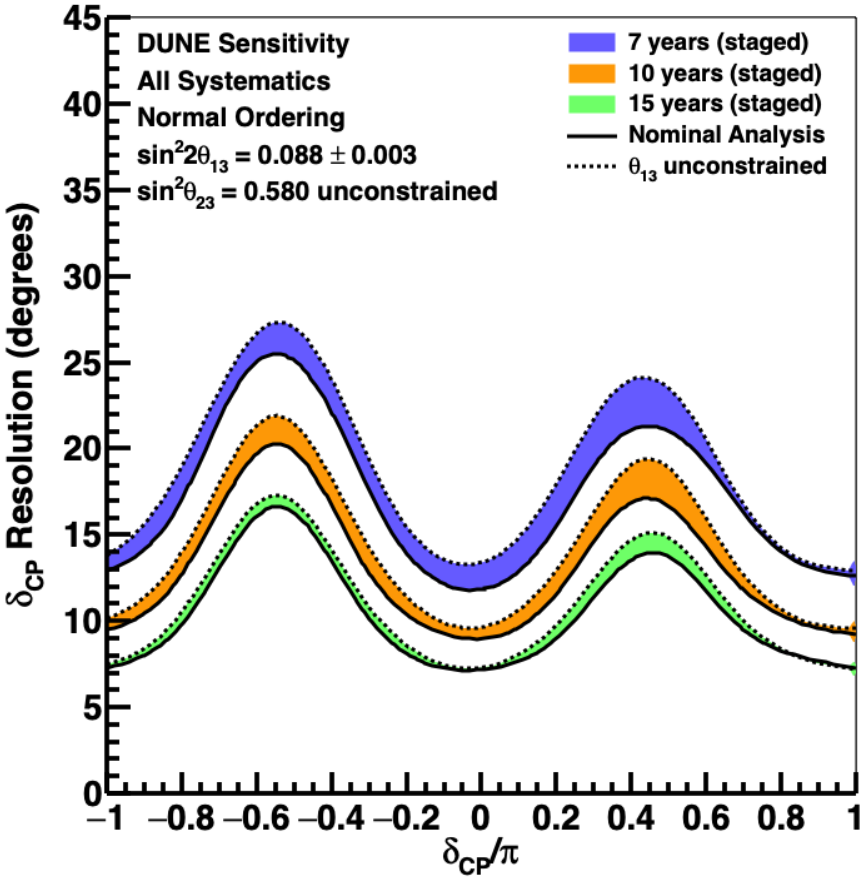


Figure 1.8: Resolution in degrees for the DUNE measurement of $\delta_{\rm CP}$, as a function of the true value of $\delta_{\rm CP}$, for seven (blue), ten (orange), and fifteen (green) years of exposure. True normal ordering is assumed. The width of the band shows the impact of applying an external constraint on $\sin^2 2\theta_{13}$.

Figures 1.9 and 1.10 show the resolution of DUNE's measurements of $\delta_{\rm CP}$ and $\sin^2 2\theta_{13}$ and of $\sin^2 2\theta_{23}$ and Δm^2_{32}, respectively, as a function of exposure in kt-MW-years. As seen in Figure 1.8, the $\delta_{\rm CP}$ resolution varies significantly with the true value of $\delta_{\rm CP}$, but for favorable values, resolutions near five degrees are possible for large exposure. The DUNE measurement of $\sin^2 2\theta_{13}$ approaches the precision of reactor experiments for high exposure, allowing a comparison between the two results, which is of interest as a test of the unitarity of the PMNS matrix.

One of the principal strengths of DUNE is its ability to simultaneously measure all oscillation parameters governing long-baseline neutrino oscillation, without a need for external constraints. As an example, Figure 1.11 shows the 90% C.L. allowed regions for $\sin^2 2\theta_{13}$ (left) and $\sin^2 \theta_{23}$ (right) versus $\delta_{\rm CP}$ for 7, 10 and 15 years of running, compared to the current measurements from world data.

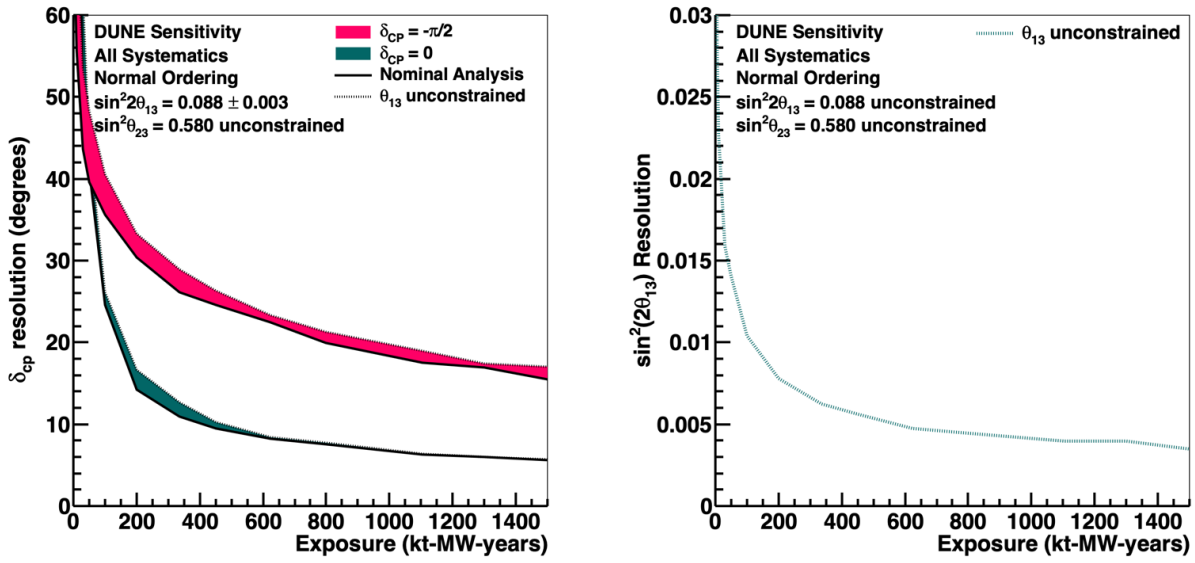


Figure 1.9: Resolution of DUNE measurements of δ_{CP} (left) and $\sin^2 2\theta_{13}$ (right), as a function of exposure in kt-MW-years. As seen in Figure 1.8, the δ_{CP} resolution has a significant dependence on the true value of δ_{CP}, so curves for $\delta_{\mathrm{CP}} = -\pi/2$ (red) and $\delta_{\mathrm{CP}} = 0$ (green) are shown. The width of the band shows the impact of applying an external constraint on $\sin^2 2\theta_{13}$. For the $\sin^2 2\theta_{13}$ resolution, an external constraint does not make sense, so only the unconstrained curve is shown. For reference, 336, 624, and 1104 kt · MW · year correspond to 7, 10, and 15 staged years, respectively.

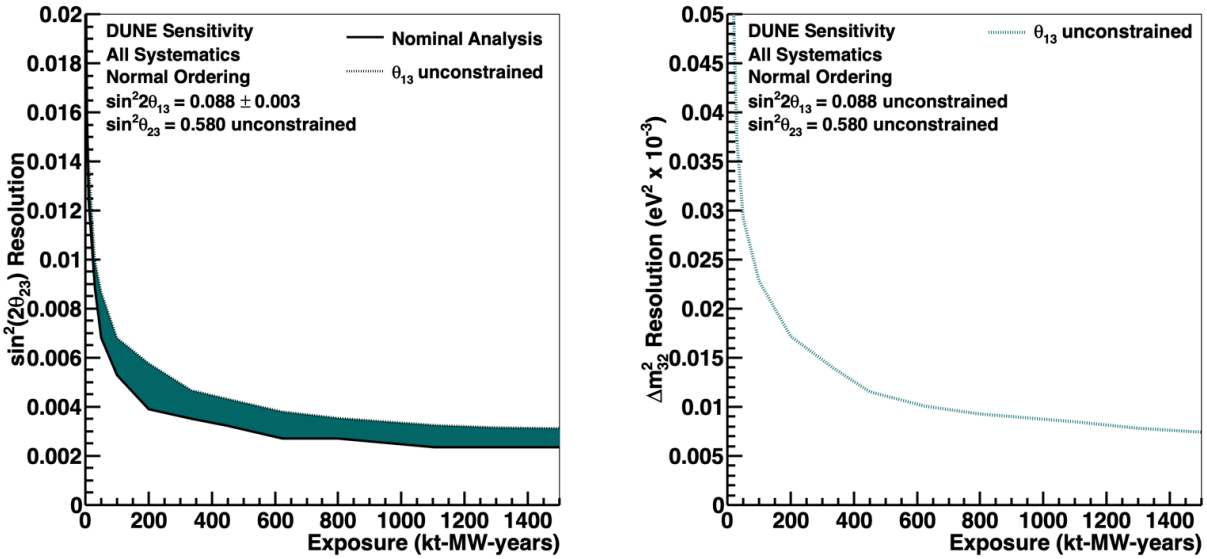


Figure 1.10: Resolution of DUNE measurements of $\sin^2 2\theta_{23}$ (left) and Δm^2_{32} (right), as a function of exposure in kt-MW-years. The width of the band for the $\sin^2 2\theta_{23}$ resolution shows the impact of applying an external constraint on $\sin^2 2\theta_{13}$. For the Δm^2_{32} resolution, an external constraint does not have a significant impact, so only the unconstrained curve is shown. For reference, 336, 624, and 1104 kt · MW · year correspond to 7, 10, and 15 staged years, respectively.

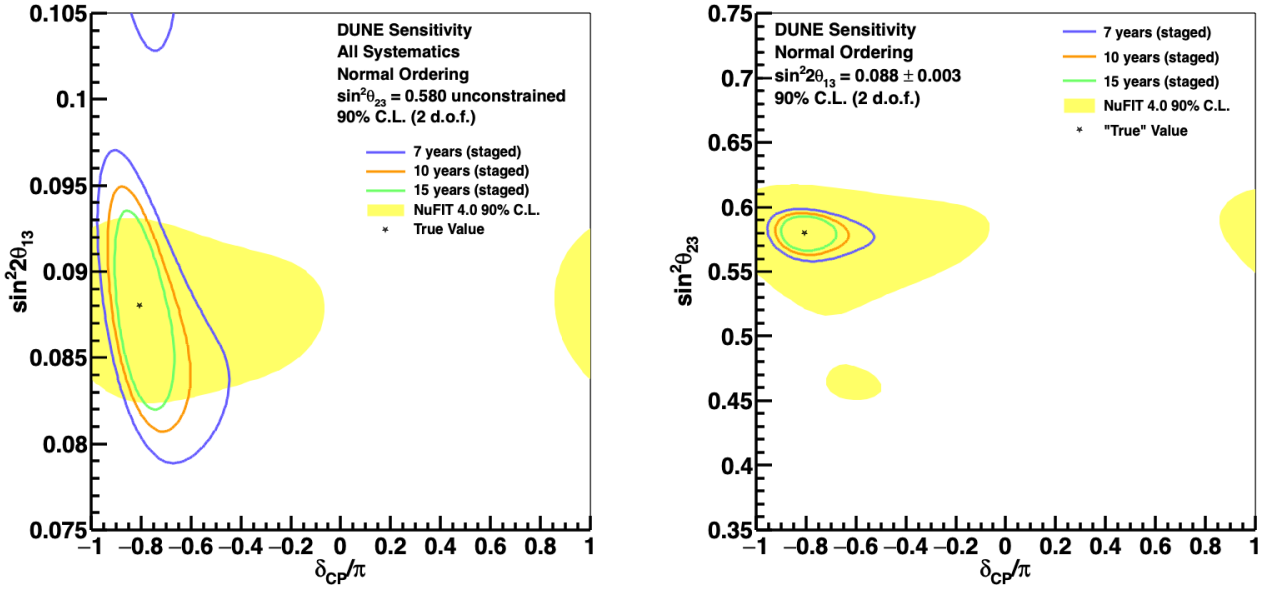


Figure 1.11: Left: Two-dimensional 90% C.L. region in $\sin^2 2\theta_{13}$ and δ_{CP}, for 7, 10, and 15 years of exposure, with equal running in neutrino and antineutrino mode. The 90% C. L. region for the NuFIT 4.0 global fit is shown in yellow for comparison. The true values of the oscillation parameters are assumed to be the central values of the NuFIT 4.0 global fit and the oscillation parameters governing long-baseline oscillation are unconstrained. Right: Corresponding region in $\sin^2 \theta_{23}$ and δ_{CP}. In this case, $\sin^2 2\theta_{13}$ is constrained by NuFIT 4.0.

The measurement of $\nu_\mu \to \nu_\mu$ oscillations is sensitive to $\sin^2 2\theta_{23}$, whereas the measurement of $\nu_\mu \to \nu_e$ oscillations is sensitive to $\sin^2 \theta_{23}$. A combination of both ν_e appearance and ν_μ disappearance measurements can probe both maximal mixing and the θ_{23} octant. Figure 1.12 shows the sensitivity to determining the octant as a function of the true value of $\sin^2 \theta_{23}$.

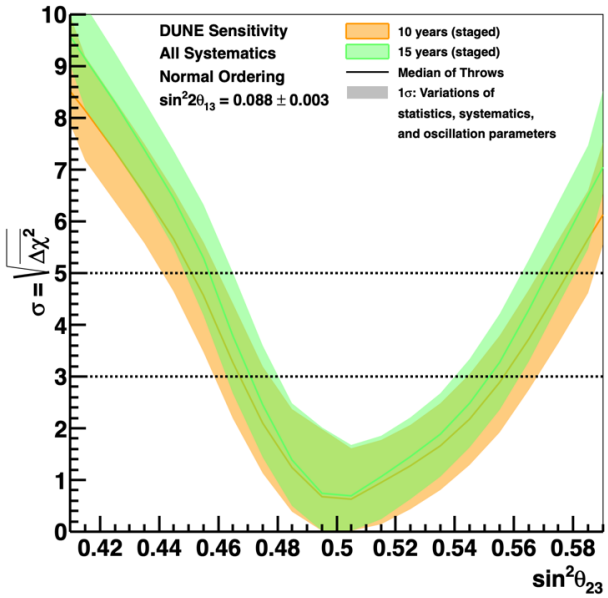


Figure 1.12: Sensitivity to determination of the θ_{23} octant as a function of the true value of $\sin^2 \theta_{23}$, for ten (orange) and fifteen (green) years of exposure. True normal ordering is assumed. The width of the transparent bands cover 68% of fits in which random throws are used to simulate statistical variations and select true values of the oscillation and systematic uncertainty parameters, constrained by pre-fit uncertainties. The solid lines show the median sensitivity.

1.3.2 Proton Decay and Other Baryon-number Violating Processes

By virtue of its deep underground location and large fiducial mass, as well as its excellent event imaging, particle identification and calorimetric capabilities, the DUNE FD will be a powerful instrument to probe baryon-number violation. DUNE will be able to observe signatures of decays of protons and neutrons, as well as the phenomenon of neutron-antineutron mixing, at rates below the limits placed by the current generation of experiments.

Many nucleon decay modes are accessible to DUNE. As a benchmark, a particularly compelling discovery channel is the decay of a proton to a positive kaon and a neutrino, $p \to K^+\overline{\nu}$. In this channel, the kaon and its decay products can be imaged, identified, and tested for kinematic consistency with the full decay chain, together with precision sufficient to reject backgrounds due to atmospheric muon and neutrino interactions. Preliminary analysis of single-particle beam and cosmic ray tracks in the ProtoDUNE-SP LArTPC is already demonstrating the particle identification capability of DUNE, as illustrated in Figure 1.13. The signature of the kaon track and its observable decay particles is sufficiently rich that a credible claim of evidence for proton decay could be made on the basis of just one or two sufficiently well-imaged events, for the case where background sources are expected to contribute much less than one event.

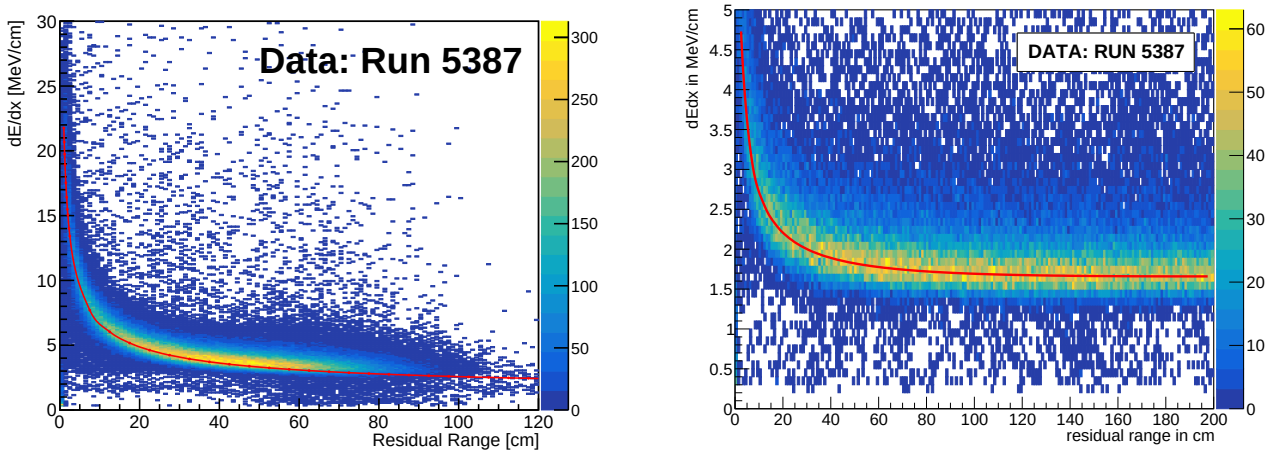


Figure 1.13: Energy loss of protons (left) and muons (right) in 1-GeV running with the ProtoDUNE-SP LArTPC at CERN, as a function of residual range. The protons are beam particles identified from beamline instrumentation; the muons are reconstructed stopping cosmic rays collected concurrently. The red curves represent the mean of the corresponding expected signature. Note the difference in the vertical scale of the two plots. The kaon dE/dx curve will lie between the two curves shown.

Projecting from the current analysis of $p \to K^+\overline{\nu}$ in the DUNE FD, with a detection efficiency of 30% as described in Volume II, DUNE Physics, Chapter 6, the expected 90% C.L. lower limit on lifetime divided by branching fraction is 1.3×10^{34} years for a $400\,\mathrm{kt} \cdot \mathrm{year}$ exposure, assuming no candidate events are observed. This is roughly twice the current limit of 5.9×10^{33} years from Super–Kamiokande [20], based on an exposure of $260\,\mathrm{kt} \cdot \mathrm{year}$. Thus, should the rate for this decay be at the current Super–Kamiokande limit, five candidate events would be expected in DUNE within ten years of running with four FD modules. Ongoing work is aimed at improving the efficiency in this and other channels.

1.3.3 Galactic Supernovae via Measurements of Neutrino Bursts

As has been demonstrated with SN1987a, the observation of neutrinos [6, 7] from a core-collapse supernova can reveal much about these phenomena that is not accessible in its electromagnetic signature. Correspondingly, there is a wide range of predictions from supernova models for even very basic characteristics of the SNBs. Typical models predict that a supernova explosion in the center of the Milky Way will result in several thousand detectable neutrino interactions in the DUNE FD occurring over an interval of up to a few tens of seconds. The neutrino energy spectrum peaks around 10 MeV, with appreciable flux up to about 30 MeV.

Liquid argon (LAr) based detectors are sensitive to the ν_e component of the flux, while water Cherenkov and organic scintillator detectors are most sensitive to the $\bar{\nu}_e$ component. Thus DUNE is uniquely positioned to study the neutronization burst, in which ν_e's are produced during the first few tens of milliseconds. More generally, measurements of the (flavor-dependent) neutrino flux and energy spectrum as a function of time over the entirety of the burst can be sensitive to astrophysical properties of the supernova and its progenitor, and distortions relative to nominal expectations can serve as signatures for phenomena such as shock wave and turbulence effects, or even black hole formation.

Below, we present the results of analyses of DUNE's capabilities for two elements of the SNB program: (1) fits to the reconstructed neutrino energy spectrum and comparison to models in which none of the distortions listed above are present, and (2) neutrino flux direction determination for angular localization of the supernova position.

1.3.3.1 Results from Fits to Pinched Thermal Neutrino Energy Spectrum

The physics of neutrino decoupling and spectra formation is far from trivial, owing to the energy dependence of the cross sections and the roles played by both CC and NC reactions. Detailed transport calculations using methods such as Monte Carlo (MC) or Boltzmann solvers have been employed. It has been observed that spectra coming out of such simulations can typically be parameterized at a given moment in time by the following ansatz (e.g., [21, 22]):

$$\phi(E_\nu) = \mathcal{N}\left(\frac{E_\nu}{\langle E_\nu\rangle}\right)^{\alpha} \exp\left[-\left(\alpha+1\right)\frac{E_\nu}{\langle E_\nu\rangle}\right] , \tag{1.7}$$

where E_ν is the neutrino energy, $\langle E_\nu\rangle$ is the mean neutrino energy, α is a "pinching parameter," and $\mathcal{N}$ is a normalization constant that can be related to the total binding energy release of the supernova, denoted ε in the discussion below. Large α corresponds to a more "pinched" spectrum (suppressed high-energy tail). This parameterization is referred to as a "pinched-thermal" form. The different ν_e, $\overline{\nu}_e$ and ν_x, $x = \mu, \tau$ flavors are expected to have different average energy and α parameters and to evolve differently in time. The primary experimental task is to determine the true neutrino spectrum from the observed supernova event spectrum. Given that the spectrum is well described by the functional form in Equation 2.7, this task is approximately equivalent to that of fitting the threepinched-thermal parameters $(\alpha^0, \langle E_\nu\rangle^0, \varepsilon^0)$ that carry the spectral information.

To evaluate DUNE's capabilities, we have developed a forward fitting algorithm requiring a binned

reconstructed neutrino energy spectrum expected for a supernova at a given distance generated with a "true" set of these parameters. Figure 1.14 shows an example of a resulting fit, with the approximate parameters for several specific supernova models superimposed to illustrate the potential for discrimination between them.

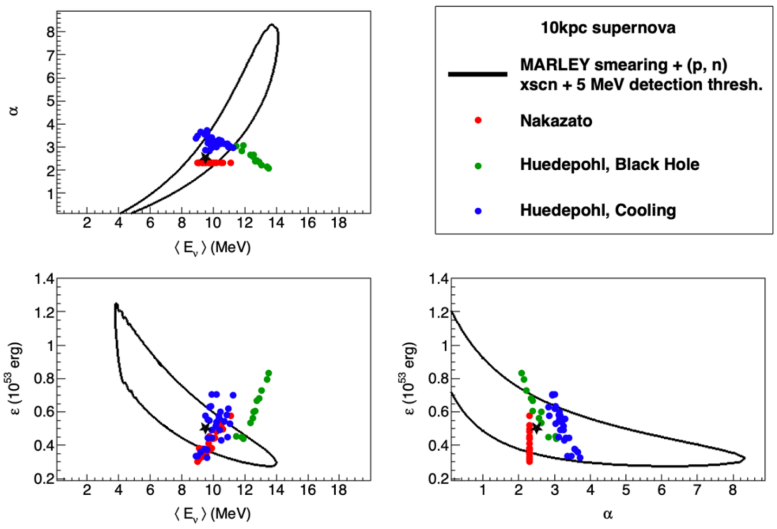


Figure 1.14: Estimated sensitivity regions for DUNE's determination of the three supernova spectra parameters at 90% C.L. given the assumed true value indicated by the black star. The simulated data were generated for a supernova at 10 kpc with a neutrino interaction model appropriate for low energies, realistic detector smearing, and a step efficiency function with a 5 MeV detected energy threshold. To indicate the expected range of possible true flux parameters, superimposed are parameters corresponding to the time-integrated flux for three different sets of models: Nakazato [23], Huedepohl black hole formation models, and Huedepohl cooling models [24]. For the Nakazato parameters (for which there is no explicit pinching, corresponding to $\alpha = 2.3$), the parameters are taken directly from the reference; for the Huedepohl models, they are fit to a time-integrated flux.

1.3.3.2 Pointing Sensitivity of DUNE

An illustration of another element of the DUNE SNB program is given in Figure 1.15, which indicates a pointing resolution of better than 5° that can be obtained by analysis of both subdominant highly-directional ν-e elastic scattering events and dominant weakly-directional ν_e CC events within a SNB, based on full reconstruction and analysis. The DUNE results can be combined with corresponding measurements in other neutrino detectors to provide supernova localization from neutrinos alone in real time.

1.3.4 Searches for Beyond-Standard-Model Physics

The unique combination of the high-intensity LBNF neutrino beam with DUNE's ND and massive LArTPC FD modules at a 1300 km baseline enables a variety of probes of BSM physics, either novel or with unprecedented sensitivity.

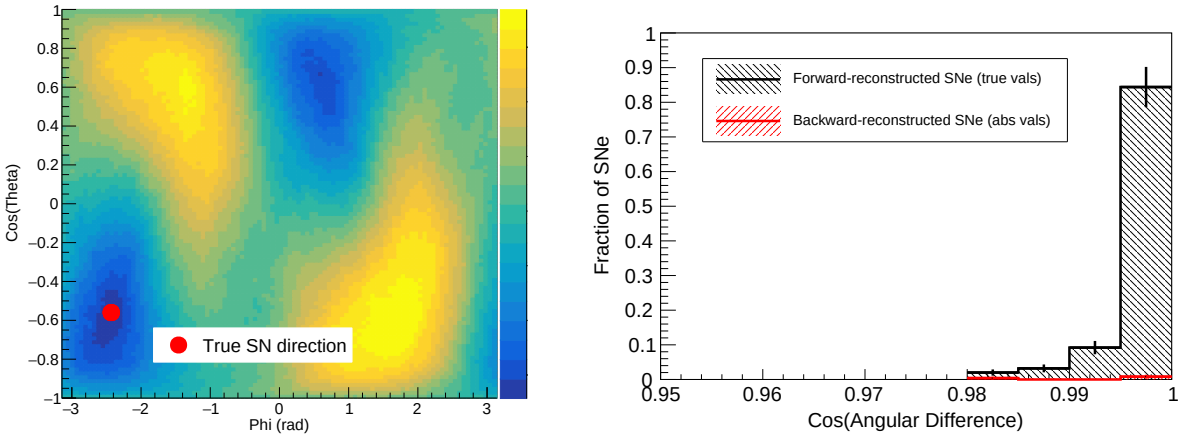


Figure 1.15: Left: Log likelihood values as a function of direction for a supernova sample with 260 ν-e elastic scattering (ES) events. Right: Distribution of angular differences for directions to 10 kpc supernova using a maximum likelihood method.

As examples of the potential impact of DUNE, we present results from the analysis of simulated data sets for two BSM scenarios, one with a sterile neutrino species participating in oscillations, and the other with anomalous "neutrino trident" events. From the sterile neutrino analysis, the DUNE sensitivities to the effective mixing angle $\theta_{\mu e}$ (which depends on new mixing angles θ_{14} and θ_{24}), from the appearance and disappearance samples at the ND and FD are shown in Figure 1.16.

Considering a neutrino trident analysis in ND data, existing constraints and projected sensitivity to parameters of a Z' boson resulting from the gauging of the difference between muon and tau lepton numbers, $L_\mu - L_\tau$, are presented in Figure 1.17. This plot indicates that DUNE can cover much of parameter space for which this model is able to explain the departure of the present observed muon $g-2$ central value from standard model expectations.

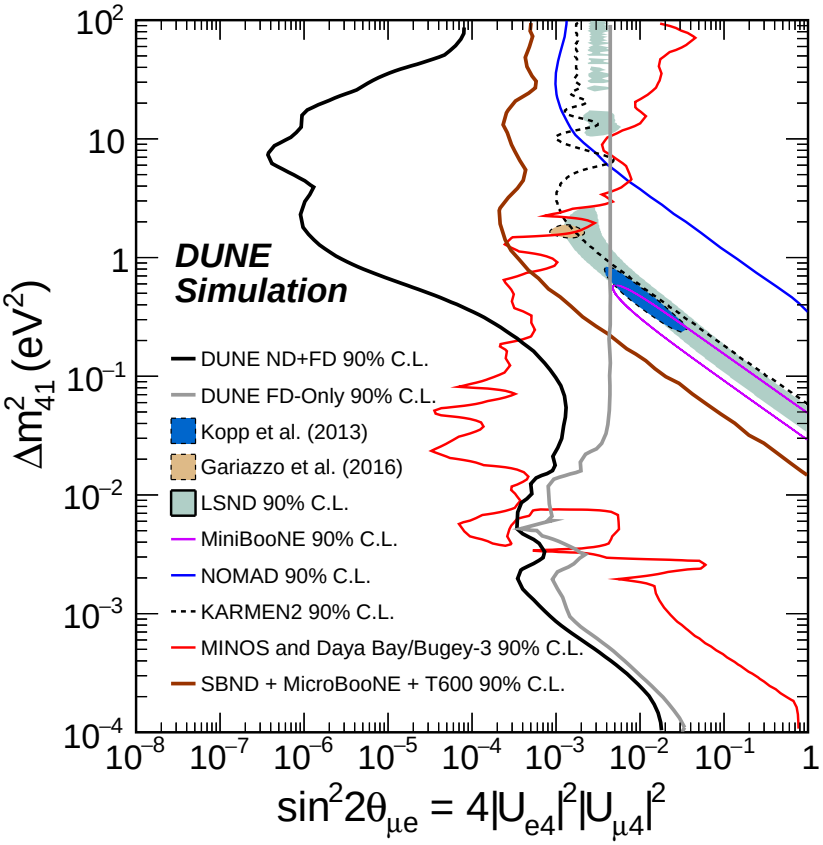


Figure 1.16: DUNE 90% C.L. sensitivities to $\theta_{\mu e}$ from the appearance and disappearance samples at the ND and FD is shown along with a comparison with previous existing experiments and the sensitivity from the future Short-Baseline Neutrino (SBN) program. Regions to the right of the DUNE contours are excluded.

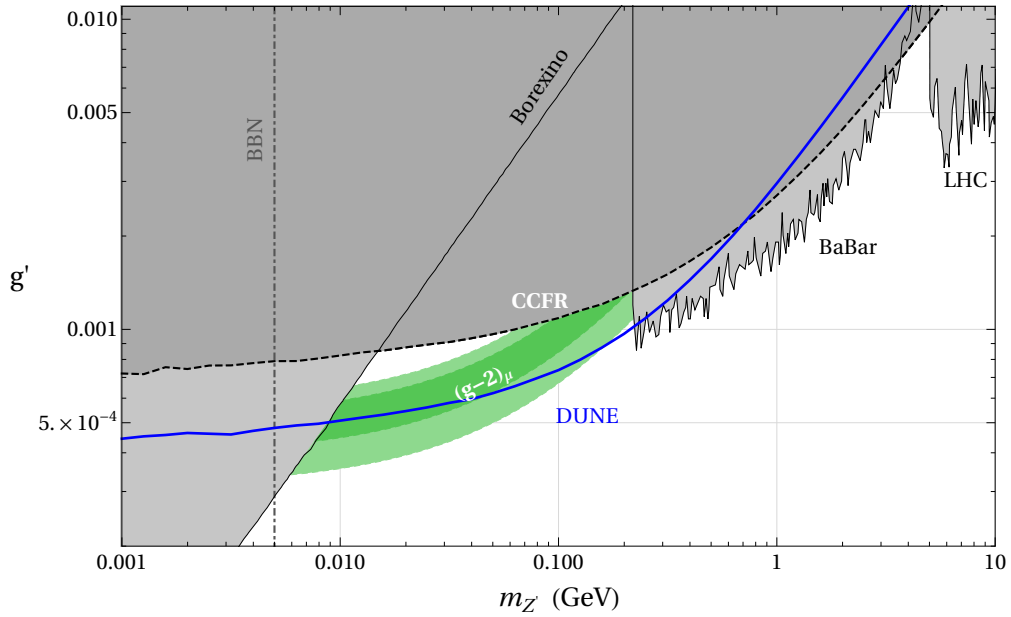


Figure 1.17: Existing constraints and projected DUNE sensitivity in the Z' parameter spaced associated with gauging $L_\mu - L_\tau$. Shown in green is the region where the $(g-2)_\mu$ anomaly can be explained at the 2σ level. The parameter regions already excluded by existing constraints are shaded in gray and correspond to a CMS search for $pp \to \mu^+\mu^- Z' \to \mu^+\mu^-\mu^+\mu^-$ [25] ("LHC"), a BaBar search for $e^+e^- \to \mu^+\mu^- Z' \to \mu^+\mu^-\mu^+\mu^-$ [26] ("BaBar"), a previous measurement of the trident cross section [27, 28] ("CCFR"), a measurement of the scattering rate of solar neutrinos on electrons [29, 30, 31] ("Borexino"), and bounds from Big Bang Nucleosynthesis [32, 33] ("BBN"). The DUNE sensitivity shown by the solid blue line assumes a measurement of the trident cross section with 40% precision.

Glossary

boosted dark matter (BDM) A new model that describes a relativistic dark matter particle boosted by the annihilation of heavier dark matter participles in the galactic center or the sun. 10

baryon-number violating (BNV) Describing an interaction where baryon number is not conserved. 6

BSM beyond the standard model. 8, 26, 27

charged current (CC) Refers to an interaction between elementary particles where a charged weak force carrier (W^+ or W^-) is exchanged. 2–4, 7, 8, 14, 15, 17, 25, 26

conceptual design report (CDR) A formal project document that describes the experiment at a conceptual level. 2, 11

European Organization for Nuclear Research (CERN) The leading particle physics laboratory in Europe and home to the ProtoDUNEs. (In French, the Organisation Européenne pour la Recherche Nucléaire, derived from Conseil Européen pour la Recherche Nucléaire. 11, 24

Cabibbo-Kobayashi-Maskawa matrix (CKM matrix) Refers to the matrix describing the mixing between mass and weak eigenstates of quarks. 3

confidence level (CL) Refers to a probability used to determine the value of a random variable given its distribution. 7

CMS Compact Muon Solenoid experiment at CERN. 29

charge parity (CP) Product of charge and parity transformations. 3, 4, 6, 17, 20

charge, parity, and time reversal symmetry (CPT) product of charge, parity and time-reversal transformations. 10

charge-parity symmetry violation (CPV) Lack of symmetry in a system before and after charge and parity transformations are applied. For CP symmetry to hold, a particle turns into its corresponding antiparticle under a charge transformation, and a parity transformation

inverts its space coordinates, i.e., produces the mirror image. 4, 5, 14, 17

dark matter (DM) The term given to the unknown matter or force that explains measurements of galaxy motion that are otherwise inconsistent with the amount of mass associated with the observed amount of photon production. 10

dual-phase (DP) Distinguishes one of the DUNE far detector technologies by the fact that it operates using argon in both gas and liquid phases. 11

Deep Underground Neutrino Experiment (DUNE) A leading-edge, international experiment for neutrino science and proton decay studies. 2, 4–8, 10–14, 17, 20, 24–27, 29

far detector (FD) The 70 kt total (40 kt fiducial) mass liquid argon time-projection chamber (LArTPC) DUNE detector, composed of four 17.5 kt total (10 kt fiducial) mass modules, to be installed at the far site at SURF in Lead, SD, USA. 2, 5, 7, 8, 10–13, 24–28

Fermi National Accelerator Laboratory (Fermilab) U.S. national laboratory in Batavia, IL. It is the laboratory that hosts Deep Underground Neutrino Experiment (DUNE) and serves as its near site. 11

final-state interactions (FSI) Refers to interactions between elementary or composite particles subsequent to the initial, fundamental particle interaction, such as may occur as the products exit a nucleus. 6

grand unified theory (GUT) A class of theories that unifies the electro-weak and strong forces. 5, 6

liquid argon (LAr) Argon in its liquid phase; it is a cryogenic liquid with a boiling point of −90 °C (87 K) and density of 1.4 g/ml. 25

liquid argon time-projection chamber (LArTPC) A time projection chamber (TPC) filled with liquid argon; the basis for the DUNE far detector (FD) modules. 6, 11, 13, 24, 26

Long-Baseline Neutrino Facility (LBNF) The organizational entity responsible for developing the neutrino beam, the cryostats and cryogenics systems, and the conventional facilities for DUNE. 4, 11, 14, 26

light-mass dark matter (LDM) Refers to dark matter particles with mass values much lower than the electroweak scale, specifically below the 1 GeV level. 10

LHC Large Hadron Collider. 10, 29

Monte Carlo (MC) Refers to a method of numerical integration that entails the statistical sampling of the integrand function. Forms the basis for some types of detector and physics

simulations. 25

neutral current (NC) Refers to an interaction between elementary particles where a neutrally charged weak force carrier (Z^0) is exchanged. 3, 7, 8, 10, 14, 15, 25

near detector (ND) Refers to the detector(s) installed close to the neutrino source at Fermilab. 2, 8, 10, 11, 13, 14, 26–28

NOvA The NOvA off-axis neutrino oscillation experiment at Fermi National Accelerator Laboratory (Fermilab). 14

nonstandard interaction (NSI) A general class of theory of elementary particles other than the Standard Model. 10

NuFIT 4.0 The NuFIT 4.0 global fit to neutrino oscillation data. 14, 22

NuMI a set of facilities at Fermilab, collectively called "Neutrinos at the Main Injector." The NuMI neutrino beamline target system converts an intense proton beam into a focused neutrino beam. 11

Pontecorvo-Maki-Nakagawa-Sakata (PMNS) A type of matrix that describes the mixing between mass and weak eigenstates of the neutrino. 3, 4, 10, 20

ProtoDUNE Either of the two DUNE prototype detectors constructed at European Organization for Nuclear Research (CERN). One prototype implements single-phase (SP) technology and the other dual-phase (DP). 11

ProtoDUNE-SP The SP ProtoDUNE detector at CERN. 24

Short-Baseline Neutrino (SBN) A Fermilab program consisting of three collaborations, MicroBooNE, SBND, and ICARUS, to perform sensitive searches for ν_e appearance and ν_μ disappearance in the Booster Neutrino Beam. 28

standard model (SM) Refers to a theory describing the interaction of elementary particles. 6, 10

supernova neutrino burst (SNB) A prompt increase in the flux of low-energy neutrinos emitted in the first few seconds of a core-collapse supernova. It can also refer to a trigger command type that may be due to this phenomenon, or detector conditions that mimic its interaction signature. 7, 13, 25, 26

single-phase (SP) Distinguishes one of the DUNE far detector technologies by the fact that it operates using argon in its liquid phase only. 11

T2K T2K (Tokai to Kamioka) is a long-baseline neutrino experiment in Japan studying neutrino oscillations. 4, 14

technical design report (TDR) A formal project document that describes the experiment at a technical level. 11, 12

weakly-interacting massive particle (WIMP) A hypothesized particle that may be a component of dark matter. 10

References

[1] **Particle Data Group** Collaboration, M. Tanabashi *et al.*, "Review of Particle Physics," *Phys. Rev.* **D98** no. 3, (2018) 030001.

[2] **T2K** Collaboration, K. Abe *et al.*, "Constraint on the Matter-Antimatter Symmetry-Violating Phase in Neutrino Oscillations," arXiv:1910.03887 [hep-ex].

[3] H. Nunokawa, S. J. Parke, and J. W. Valle, "CP Violation and Neutrino Oscillations," *Prog.Part.Nucl.Phys.* **60** (2008) 338–402, arXiv:0710.0554 [hep-ph].

[4] **LBNE** Collaboration, M. Bass *et al.*, "Baseline optimization for the measurement of CP violation, mass hierarchy, and θ_{23} octant in a long-baseline neutrino oscillation experiment," *Phys.Rev.* **D91** no. 5, (2015) 052015, arXiv:1311.0212 [hep-ex].

[5] K. S. Babu *et al.*, "Working Group Report: Baryon Number Violation," in *Proceedings, 2013 Community Summer Study on the Future of U.S. Particle Physics: Snowmass on the Mississippi (CSS2013): Minneapolis, MN, USA, July 29-August 6, 2013*. 2013. arXiv:1311.5285 [hep-ph]. http://www.slac.stanford.edu/econf/C1307292/docs/IntensityFrontier/BaryonNo-13.pdf.

[6] R. Bionta, G. Blewitt, C. Bratton, D. Casper, A. Ciocio, *et al.*, "Observation of a Neutrino Burst in Coincidence with Supernova SN 1987a in the Large Magellanic Cloud," *Phys.Rev.Lett.* **58** (1987) 1494.

[7] **KAMIOKANDE-II** Collaboration, K. Hirata *et al.*, "Observation of a Neutrino Burst from the Supernova SN 1987a," *Phys.Rev.Lett.* **58** (1987) 1490–1493.

[8] D. N. Schramm and J. W. Truran, "New physics from Supernova SN1987A," *Phys. Rept.* **189** (1990) 89–126.

[9] F. Vissani, "Comparative analysis of SN1987A antineutrino fluence," *J. Phys.* **G42** (2015) 013001, arXiv:1409.4710 [astro-ph.HE].

[10] A. Mirizzi, I. Tamborra, H.-T. Janka, N. Saviano, K. Scholberg, R. Bollig, L. Hudepohl, and S. Chakraborty, "Supernova Neutrinos: Production, Oscillations and Detection," *Riv. Nuovo Cim.* **39** no. 1-2, (2016) 1–112, arXiv:1508.00785 [astro-ph.HE].

[11] S. Horiuchi and J. P. Kneller, "What can be learned from a future supernova neutrino detection?," *J. Phys.* **G45** no. 4, (2018) 043002, arXiv:1709.01515 [astro-ph.HE].

[12] L. Hudepohl, B. Muller, H.-T. Janka, A. Marek, and G. Raffelt, "Neutrino Signal of Electron-Capture Supernovae from Core Collapse to Cooling," *Phys.Rev.Lett.* **104** (2010) 251101, arXiv:0912.0260 [astro-ph.SR].

[13] K. Scholberg, "Supernova Neutrino Detection," *Ann.Rev.Nucl.Part.Sci.* **62** (2012) 81–103, arXiv:1205.6003 [astro-ph.IM].

[14] I. Esteban, M. C. Gonzalez-Garcia, A. Hernàndez-Cabezudo, M. Maltoni, and T. Schwetz, "Global analysis of three-flavour neutrino oscillations: synergies and tensions in the determination of θ_{23}, δ_{CP}, and the mass ordering," arXiv:1811.05487 [hep-ph].

[15] "Nufit4.0." http://www.nu-fit.org/.

[16] P. F. de Salas, D. V. Forero, C. A. Ternes, M. Tortola, and J. W. F. Valle, "Status of neutrino oscillations 2018: 3σ hint for normal mass ordering and improved CP sensitivity," *Phys. Lett.* **B782** (2018) 633–640, arXiv:1708.01186 [hep-ph].

[17] F. Capozzi, E. Lisi, A. Marrone, D. Montanino, and A. Palazzo, "Status and prospects of global analyses of neutrino mass-mixing parameters," *J. Phys. Conf. Ser.* **888** no. 1, (2017) 012037.

[18] **NOvA** Collaboration, M. A. Acero *et al.*, "First Measurement of Neutrino Oscillation Parameters using Neutrinos and Antineutrinos by NOvA," *Phys. Rev. Lett.* **123** no. 15, (2019) 151803, arXiv:1906.04907 [hep-ex].

[19] **T2K** Collaboration, K. Abe *et al.*, "Search for CP Violation in Neutrino and Antineutrino Oscillations by the T2K Experiment with 2.2×10^{21} Protons on Target," *Phys. Rev. Lett.* **121** no. 17, (2018) 171802, arXiv:1807.07891 [hep-ex].

[20] **Super-Kamiokande** Collaboration, K. Abe *et al.*, "Search for proton decay via $p \to \nu K^+$ using 260 kiloton-year data of Super-Kamiokande," *Phys. Rev.* **D90** no. 7, (2014) 072005, arXiv:1408.1195 [hep-ex].

[21] H. Minakata, H. Nunokawa, R. Tomas, and J. W. Valle, "Parameter Degeneracy in Flavor-Dependent Reconstruction of Supernova Neutrino Fluxes," *JCAP* **0812** (2008) 006, arXiv:0802.1489 [hep-ph].

[22] I. Tamborra, B. Muller, L. Hudepohl, H.-T. Janka, and G. Raffelt, "High-resolution supernova neutrino spectra represented by a simple fit," *Phys.Rev.* **D86** (2012) 125031, arXiv:1211.3920 [astro-ph.SR].

[23] K. Nakazato, K. Sumiyoshi, H. Suzuki, T. Totani, H. Umeda, and S. Yamada, "Supernova Neutrino Light Curves and Spectra for Various Progenitor Stars: From Core Collapse to Proto-neutron Star Cooling," *Astrophys. J. Suppl.* **205** (2013) 2, arXiv:1210.6841

[astro-ph.HE].

[24] L. Huedepohl, *Neutrinos from the Formation, Cooling and Black Hole Collapse of Neutron Stars*. PhD thesis, Technische Universitat Munchen., 2014. https://wwwmpa.mpa-garching.mpg.de/ccsnarchive/data/Huedepohl2014_phd_thesis/.

[25] **CMS** Collaboration, A. M. Sirunyan *et al.*, "Search for an $L_\mu - L_\tau$ gauge boson using Z$\to 4\mu$ events in proton-proton collisions at $\sqrt{s} = 13$ TeV," *Submitted to: Phys. Lett.* (2018) , arXiv:1808.03684 [hep-ex].

[26] **BaBar** Collaboration, J. P. Lees *et al.*, "Search for a muonic dark force at BABAR," *Phys. Rev. D* **94** no. 1, (2016) 011102, arXiv:1606.03501 [hep-ex].

[27] **CCFR** Collaboration, S. R. Mishra *et al.*, "Neutrino tridents and W Z interference," *Phys. Rev. Lett.* **66** (1991) 3117–3120.

[28] W. Altmannshofer, S. Gori, M. Pospelov, and I. Yavin, "Neutrino Trident Production: A Powerful Probe of New Physics with Neutrino Beams," *Phys. Rev. Lett.* **113** (2014) 091801, arXiv:1406.2332 [hep-ph].

[29] G. Bellini *et al.*, "Precision measurement of the 7Be solar neutrino interaction rate in Borexino," *Phys. Rev. Lett.* **107** (2011) 141302, arXiv:1104.1816 [hep-ex].

[30] R. Harnik, J. Kopp, and P. A. N. Machado, "Exploring nu Signals in Dark Matter Detectors," *JCAP* **1207** (2012) 026, arXiv:1202.6073 [hep-ph].

[31] **Borexino** Collaboration, M. Agostini *et al.*, "First Simultaneous Precision Spectroscopy of *pp*, ^{7}Be, and *pep* Solar Neutrinos with Borexino Phase-II," arXiv:1707.09279 [hep-ex].

[32] B. Ahlgren, T. Ohlsson, and S. Zhou, "Comment on 'Is Dark Matter with Long-Range Interactions a Solution to All Small-Scale Problems of Λ Cold Dark Matter Cosmology?'," *Phys. Rev. Lett.* **111** no. 19, (2013) 199001, arXiv:1309.0991 [hep-ph].

[33] A. Kamada and H.-B. Yu, "Coherent Propagation of PeV Neutrinos and the Dip in the Neutrino Spectrum at IceCube," *Phys. Rev. D* **92** no. 11, (2015) 113004, arXiv:1504.00711 [hep-ph].